Chemical Science

ROYAL SOCIETY OF CHEMISTRY

EDGE ARTICLE

View Article Online
View Journal | View Issue

Cite this: *Chem. Sci.*, 2020, **11**, 2243

All publication charges for this article have been paid for by the Royal Society of Chemistry

Stable group 8 metal porphyrin mono- and bis(dialkylcarbene) complexes: synthesis, characterization, and catalytic activity†

Hai-Xu Wang, [a] Qingyun Wan, [a] Kam-Hung Low, [a] Cong-Ying Zhou, [ac] Jie-Sheng Huang, [a] Jun-Long Zhang [d] and Chi-Ming Che *[ab]

Alkyl-substituted carbene (CHR or CR_2, R = alkyl) complexes have been extensively studied for alkylcarbene (CHR) ligands coordinated with high-valent early transition metal ions (a.k.a. Schrock carbenes or alkylidenes), yet dialkylcarbene (CR_2) complexes remain less developed with bis(dialkylcarbene) species being little (if at all) explored. Herein, several group 8 metal porphyrin dialkylcarbene complexes, including Fe- and Ru-mono(dialkylcarbene) complexes [M(Por)(Ad)] (**1a,b**, M = Fe, Por = porphyrinato dianion, Ad = 2-adamantylidene; **2a,b**, M = Ru) and Os-bis(dialkylcarbene) complexes [Os(Por)$(Ad)_2$] (**3a–c**), are synthesized and crystallographically characterized. Detailed investigations into their electronic structures reveal that these complexes are formally low-valent M(II)-carbene in nature. These complexes display remarkable thermal stability and chemical inertness, which are rationalized by a synergistic effect of strong metal-carbene covalency, hyperconjugation, and a rigid diamondoid carbene skeleton. Various spectroscopic techniques and DFT calculations suggest that the dialkylcarbene Ad ligand is unique compared to other common carbene ligands as it acts as both a potent σ-donor and π-acceptor; its unique electronic and structural features, together with the steric effect of the porphyrin macrocycle, make its Fe porphyrin complex **1a** an active and robust catalyst for intermolecular diarylcarbene transfer reactions including cyclopropanation (up to 90% yield) and X–H (X = S, N, O, C) insertion (up to 99% yield) reactions.

Received 28th October 2019
Accepted 30th December 2019

DOI: 10.1039/c9sc05432d

rsc.li/chemical-science

Introduction

Since the discovery of a metal-alkylcarbene (M=CHR) complex, [Ta($CH_2{}^tBu)_3$($CH{}^tBu$)], by Schrock,[1] alkyl-substituted carbene ligands (alternative name: alkylidenes), *i.e.*, alkylcarbene (CHR) and dialkylcarbene (CR_2), have been mainly studied for M=CHR complexes with early transition metals (TMs, groups 4–6), with their roles ranging from reactive synthons in olefin metathesis to supporting ligands (in nucleophilic, dianionic form $(CHR)^{2-}$) that stabilize high-valent metal ions.[2] In contrast, the chemistry of dialkylcarbene complexes of TMs and CHR/CR_2 complexes of middle/late TMs remains less developed (Fig. 1a), particularly for mononuclear bis(CHR/CR_2) complexes, examples of which are sparse.[3] To the best of our knowledge, no mononuclear bis(dialkylcarbene) complexes of TMs have been reported previously.[4]

We are interested in developing new types of dialkylcarbene complexes of group 8 metals Fe, Ru, and Os. In the literature, Grubbs' Ru-alkylcarbene species have received much attention owing to their essential role in olefin metathesis.[5] Related CHR/CR_2 species of Fe,[6] Ru,[7] and Os,[3d,8] mostly stabilized by strong-field ligands such as CO/phosphine and Cp (cyclopentadienyl), have also been reported; some Fe-(di)alkylcarbene complexes $[Cp(CO)(L)Fe(CHR)]^+$ (L = PR_3, CO)[9] or $[Cp(CO)_2Fe(CR_2)]^+$[10] undergo stoichiometric reactions typical of electrophilic carbenes, including cyclopropanation,[9a–g,10] Si–H insertion,[9h] and C–H insertion.[9i] Interest in Fe-carbene complexes[6a,11] also lies in their potential role as next-generation catalysts for olefin metathesis and mechanistic implication of iron porphyrin carbene complexes for artificial metalloenzyme catalysis involving heme-carbenes as key intermediates.[12] Recently, we developed catalytic dialkylcarbene transfer reactions[13] including C(sp^3)–H insertion, cyclopropanation, and Buchner reactions using various metalloporphyrin catalysts including Ru and Fe porphyrins; the active intermediates in these catalytic processes

[a]*State Key Laboratory of Synthetic Chemistry, Department of Chemistry, The University of Hong Kong, Pokfulam Road, Hong Kong SAR, China. E-mail: cmche@hku.hk*
[b]*HKU Shenzhen Institute of Research & Innovation, Shenzhen, China*
[c]*College of Chemistry and Materials Science, Jinan University, Guangzhou, China*
[d]*Beijing National Laboratory for Molecular Sciences, College of Chemistry and Molecular Engineering, Peking University, Beijing, China*

† Electronic supplementary information (ESI) available: Abbreviations, experimental procedures, characterization of compounds, computational details, Tables S1–S8, Fig. S1–S11, NMR spectra of compounds, Cartesian coordinates from DFT calculations, and CIF file for the crystal structure of **1b**, **1a**·Py, **2b**·MeOH, **2az**, and **3a**. CCDC: 1854823, 1854830, 1943318, 1943319, and 1943321. For ESI and crystallographic data in CIF or other electronic format see DOI: 10.1039/c9sc05432d

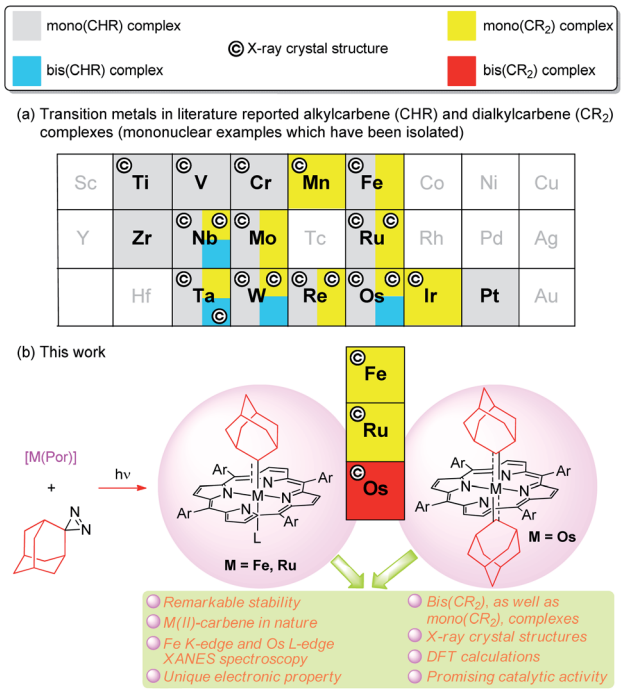

Fig. 1 (a) Literature examples of isolated mononuclear (di)alkylcarbene complexes of TMs. Mono- and bis(CHR/CR_2) complexes are represented by different colors filled. Structurally characterized examples are indicated by ©. TMs for which no isolated examples were found are left blank. (b) Group 8 metal porphyrin dialkylcarbene complexes reported in this work. M=Ad (M = Fe, Ru, Os) represents an Ad → M σ bonding (–) and a M → Ad π-backbonding (---).

are likely to be the corresponding metalloporphyrin dialkylcarbene complexes [M(Por)(CR_2)] (Por = porphyrinato dianion), which, however, have not been directly detected. Unlike the above-mentioned $[Cp(CO)(L)Fe(CHR)]^+$ and $[Cp(CO)_2Fe(CR_2)]^+$ which bear strong π-acidic CO ligand(s) in favor of low-valent metal centers, complexes [M(Por)(CR_2)] can possibly be formulated as either low-valent $M^{II}\leftarrow(:CR_2)^0$ or high-valent $M^{IV}{=}(CR_2)^{2-}$ species.[14] To clarify this issue, it is highly desirable to isolate and fully characterize stable metalloporphyrin dialkylcarbene complexes for detailed studies on their electronic and molecular structures.

Up to now, metalloporphyrin dialkylcarbene complexes have been rarely reported; the only examples are [Fe(TPP)(CMeR)] (R = ^{n}Bu, ^{n}Pr) prepared by treatment of [Fe(TPP)Cl] with terminal alkynes and $NaBH_4$.[15] These [Fe(TPP)(CMeR)] complexes were not structurally characterized by X-ray crystallography and were formulated as Fe(II) species by analogy with the ^{1}H NMR, UV-vis, and MS spectra of iron porphyrins bearing other types of carbene ligands. The very limited knowledge on metalloporphyrin dialkylcarbene species contrasts with extensive studies on other types of nonheteroatom-stabilized carbene complexes of Fe,[11e,16] Ru,[7a,17] and Os[18] porphyrins, which were generally prepared using diazo compounds as carbene sources; such a synthetic method is hardly applicable to dialkylcarbene complexes owing to the short lifetime of dialkyldiazomethanes. Moreover, metalloporphyrin dialkylcarbene species could be prone to undergo a 1,2-hydride shift, which is a common side reaction observed in dialkylcarbene transfer catalysis.[13] In addition, non-porphyrin group 8 metal dialkylcarbene complexes reported previously were often prepared with a limited choice of ligand sets (*e.g.*, phosphine, Cp, and tris(pyrazolyl)borate) and/or under demanding conditions (*e.g.*, strong acid and reducing medium),[5–8] and only a few non-porphyrin Ru-[7b–e,19] and Os-dialkylcarbene[20] complexes have been structurally characterized by X-ray crystallographic studies and, despite the report of a structurally characterized Fe=CHMe non-porphyrin complex,[21] no crystal structure of an Fe-dialkylcarbene complex has been reported so far.

In quest of a highly stable dialkylcarbene complex of metalloporphyrins, we paid attention to the dialkylcarbene ligand 2-adamantylidene (Ad). This was inspired by the studies of Ad as a model of dialkylcarbene in free carbene chemistry, as it can be photochemically generated from the diazirine compound, aziadamantane, under mild conditions and exhibits great resistance against 1,2-hydride shift due to its rigid diamondoid skeleton,[22] coupled with the use of diazirines as carbene sources for the preparation of non-porphyrin metal-C(Ph)X (X = OMe, Br) carbene complexes;[23] there is a literature report on the X-ray crystal structure of $[Cp(CO)_2Mn(Ad)]$,[24] which is hitherto the only example of a known M=Ad complex, although this Mn=Ad complex was prepared from a metal-borylene precursor rather than using aziadamantane as the Ad source. We envisaged that diazirines could be a new type of carbene source for synthesizing metal-dialkylcarbene species and Ad may also lead to isolable group 8 metal porphyrin dialkylcarbene complexes by reaction of readily accessible metalloporphyrin precursors with aziadamantane under photolysis.

In the present work, we report a simple and mild method of synthesizing dialkylcarbene complexes of TMs using diazirine as the carbene source, leading to the isolation of several M=Ad complexes of group 8 metal porphyrins including Fe- and Ru-mono(dialkylcarbene) [M(Por)(Ad)] (M = Fe **1**, Ru **2**) and Os-bis(dialkylcarbene) $[Os(Por)(Ad)_2]$ (**3**) complexes, along with the X-ray crystal structures of these complexes, as well as various spectroscopic studies including XANES (X-ray absorption near edge structure) spectroscopy and also DFT calculations (Fig. 1b), which all lend evidence for the low-valent M(II)-carbene nature of **1–3**. Complexes **3a–c** contribute unique examples of a bis(dialkylcarbene) complex of TMs. Surprisingly, the metal-dialkylcarbene complexes **1–3** are not reactive toward dialkylcarbene transfer reactions and generally display remarkable stability. Direct comparison is also made among dialkylcarbene Ad and other types of carbene ligands, mainly based on the system of group 8 metal porphyrins. Furthermore, a promising role of dialkylcarbene Ad as a supporting ligand is demonstrated by one of its Fe complexes **1a** in homogeneous donor–donor carbene transfer catalysis.

Results

Synthetic procedures

Treatment of $[Fe^{II}(TPFPP)]$ and aziadamantane at room temperature under UV irradiation (365 nm) for 15 min afforded

1a in 93% yield as a bright red solid (reaction 1 in Scheme 1a). Alternatively, it could be synthesized directly from commercially available [Fe^{III}(TPFPP)Cl] at 40 °C with a slightly lower yield (85%, reaction 2 in Scheme 1a; the Fe(III) center was presumably reduced *in situ* by free Ad). Complex [Fe(TTP)(Ad)] (**1b**) could be prepared by the same two methods yet in much lower isolated yields, probably due to its higher susceptibility to aerobic oxidation as it decomposed immediately to μ-oxo dimer [Fe(TTP)]$_2$O at above 60 °C in air (reaction 4 in Scheme 1a). Six-coordinate iron porphyrin carbene species **1a**·Py could be easily accessed by adding pyridine into a solution of **1a** (reaction 3 in Scheme 1a). Ruthenium analogues [Ru(Por)(Ad)] (Por = TPFPP: **2a**; TTP: **2b**) could be similarly prepared from [Ru^{II}(Por)(CO)] and aziadamantane in high yields (reaction 5 in Scheme 1b). Besides **2a,b**, diazirine complexes **2az** and **2bz** (Scheme 1b), which are a new class of metalloporphyrin complexes, were isolated as minor species. The coordinated diazirine molecules are less photoactive and **2az** could only be sluggishly transformed into **2a** under UV irradiation and at elevated temperature (reaction 6 in Scheme 1b); we conceive that the coordinated diazirine ligand was either first converted to the corresponding diazo compound which then reacted with Ru porphyrin, or directly decomposed to free carbene that subsequently coordinated to the Ru center. Complexes **2az** and **2bz** were also slightly air-sensitive and slowly underwent oxidation to give 2-adamantanone.[25]

Strikingly, by a similar treatment of [Os(Por)(CO)] (Por = 4-F-TPP, TPFPP, and TTP) with aziadamantane, bis(dialkylcarbene) products [Os(Por)(Ad)$_2$] (Por = 4-F-TPP: **3a**, TPFPP: **3b**, and TTP: **3c**) were observed by ^{1}H NMR measurements (reaction 7 in Scheme 1c). Monitoring the reaction of [Os(TPFPP)(CO)] and aziadamantane by ^{1}H NMR showed that **3b** was formed immediately after UV irradiation and no mono(dialkylcarbene) species [Os(Por)(Ad)] was detected. Thus it is likely that the bis(dialkylcarbene) complexes **3a–c** were formed directly from the Os carbonyl precursors, different from the pre-formation of an isolable mono(diarylcarbene) analogue [Os(TPFPP)(CPh$_2$)] and its conversion to the bis(diarylcarbene) counterpart [Os(TPFPP)(CPh$_2$)$_2$].[18e] Besides, **3a–c** could all be readily purified by using an alumina column in air, in contrast to the analogous bis(diarylcarbene) complexes which could not be isolated in a pure form when supported by simple porphyrin ligands such as TTP.[18a,d] The lower isolated yields (12–30%) for **3a–c** are attributable to the strong absorptivity of the Os precursors at 365 nm; attempts to improve the yields of **3a–c** by increasing irradiation time were not successful, as prolonged irradiation caused

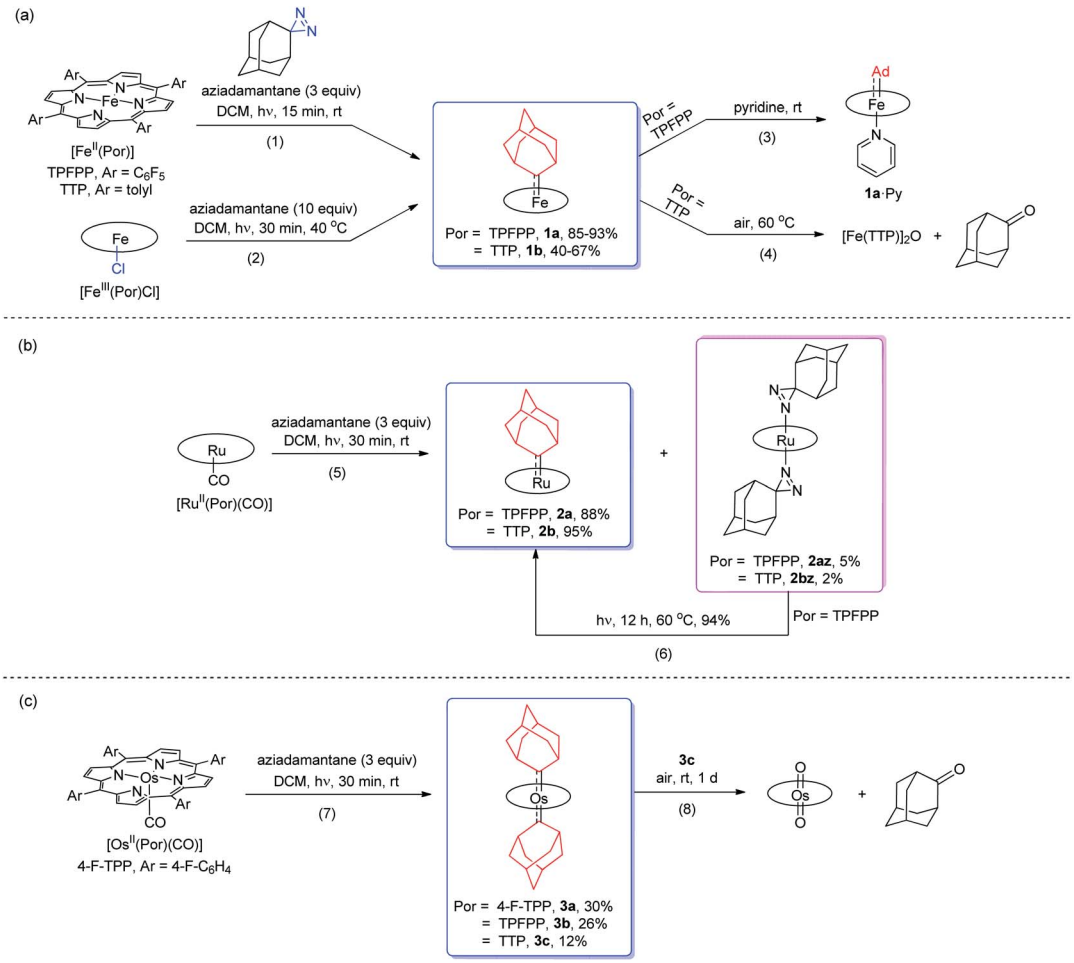

Scheme 1 Synthesis of Fe (a), Ru (b), and Os (c) dialkylcarbene complexes.

decomposition of the Os-dialkylcarbene products. The bis(dialkylcarbene) complexes **3a–c** were found slightly susceptible to aerobic oxidation, as exemplified by the oxidation of **3c** to a *trans*-dioxo complex [Os(TTP)O_2] and 2-adamantanone after standing in aerobic solution for ~1 d (reaction 8 in Scheme 1c).

X-ray crystallography

The crystal structures of **1b**, **1a**·Py, **2b**·MeOH, and **3a** were determined by X-ray crystallography (Fig. 2), and the selected bond distances and angles are listed in Table 1. The sum of angles around $C_{carbene}$ atoms (**1b**: 360.1°; **1a**·Py: 359.9°; **2b**·MeOH: 359.9°; **3a**: 359.8°) is indicative of sp^2-hybridization of carbene carbons; the carbene planes are close to bisecting the M–$N_{pyrrole}$ bonds (31.6–44.3°) in all four complexes. The Fe–$C_{carbene}$ distance in **1b** is 1.770(3) Å, which is typical of five-coordinate iron porphyrin carbene species.[11e,16a] The TTP macrocycle suffers from saddled distortion and the mean deviation of 24 atoms from the porphyrin mean plane is 0.268 Å, with the iron atom being displaced from this mean plane by 0.269 Å. Coordination of pyridine at the *trans* axial site causes elongation of the Fe–$C_{carbene}$ distance to 1.829(9) Å in **1a**·Py, yet this distance is still much shorter than Fe–C single bonds;[26] meanwhile, distortion of the porphyrin ligand is greatly suppressed (mean deviation: 0.051 Å) and the iron atom is only marginally deviated (0.074 Å) from the mean porphyrin plane. The crystal structure of **2b**·MeOH features a short Ru–$C_{carbene}$ distance of 1.856(3) Å, and its porphyrin ring shows a minor doming distortion (mean deviation: 0.037 Å) along with a slightly out-of-plane Ru atom (0.172 Å).

The Os–bis(dialkylcarbene) complex **3a** features an Os–$C_{carbene}$ bond length of 2.061(7) Å, similar to the bis(diphenylcarbene) complex [Os(TPFPP)(CPh_2)$_2$] (~2.03 Å)[18e] yet apparently longer than that of Os porphyrin mono(carbene) complexes (1.79–1.87 Å),[18c,e] which is likely due to the strong *trans* influence exerted by the carbene ligands. A 90° disorder is observed for one of the two Ad ligands, making them either orthogonal or parallel to each other. Notably, the porphyrin plane in **3a** is almost planar (mean deviation: 0.025 Å), which is in stark contrast to the strongly ruffled porphyrin ligand observed in [Os(TPFPP)(CPh_2)$_2$] (mean deviation: 0.197 Å).[18e]

Table 1 Selected bond lengths (Å) and angles (°)

(M = Fe, Ru, Os)	**1b**	**1a**·Py	**2b**·MeOH	**3a**[a]
M1–C1	1.770(3)	1.829(9)	1.856(3)	2.061(7)
C1–C2	1.500(4)	1.50(3)	1.511(5)	1.510(7)
C1–C3	1.488(5)	1.50(2)	1.507(5)	1.510(7)
M1–$N_{pyrrole}$[b]	1.978(4)	1.996(8)	2.047(3)	2.065(5)
M1–L_{ax}[c]		2.200(8)	2.364(3)	2.061(7)
C2–C1–C3	112.8(3)	111.2(12)	110.7(3)	106.8(7)
C2–C1–M1	124.2(2)	123.2(11)	124.5(2)	126.3(6)
C3–C1–M1	123.1(2)	125.5(11)	124.7(2)	126.7(5)
C1–M1–L_{ax}[c]		178.4(7)	176.16(12)	180.0(9)

[a] All values involving C1–3 are averaged between two Ad groups. [b] Average distances between M1 and pyrrolic nitrogens (N1–4). [c] L_{ax} = N5 (for **1a**·Py) or O1 (for **2b**·MeOH), or C1a (for **3a**).

Complexes **2az** and **2bz** represent two of rare examples of metal diazirine complexes[25,27] and the X-ray crystal structure of **2az** was obtained (Fig. 3). The two diazirine moieties experience slight π-backbonding from the Ru center, as the N=N bond distance (1.248(9) Å) is longer than those in non-coordinated diazirines (1.228–1.235 Å)[25] while the Ru–$N_{diazirine}$ bonds (1.985(6) and 1.996(6) Å) are also shorter than a typical Ru–N single bond (~2.1 Å). Evidence of such π-backbonding further comes from the N=N stretching bands observed in the IR spectrum of **2az** (1518 and 1491 cm^{-1}) which appear at appreciably lower frequencies than that of the free ligand (1570 cm^{-1}).[28]

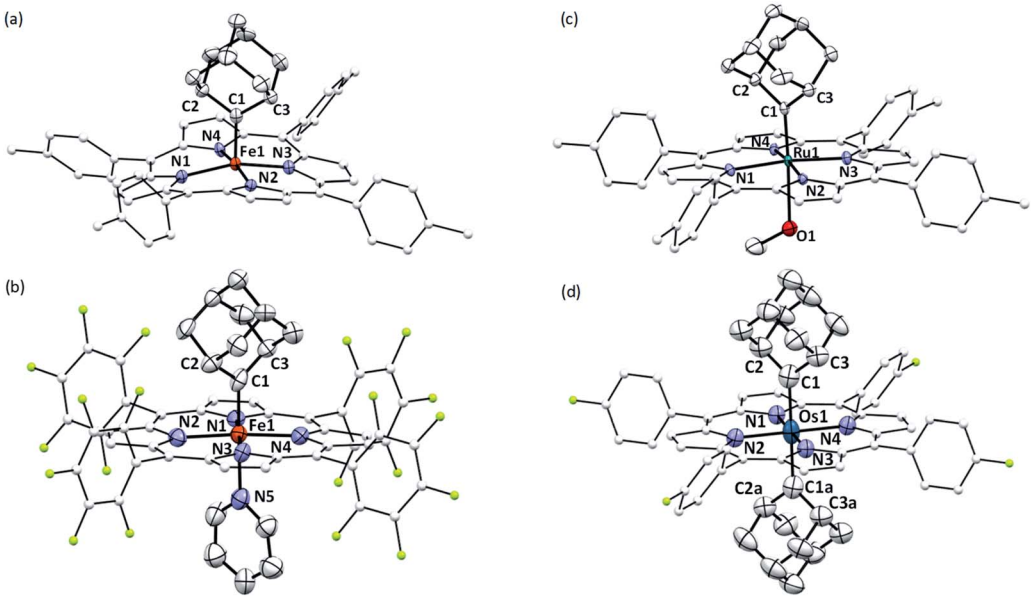

Fig. 2 ORTEP diagrams of **1b** (a), **1a**·Py (b), **2b**·MeOH (c), and **3a** (d) with thermal ellipsoids at the 50% probability level. Hydrogen atoms, disordered atoms/solvent molecules, and ellipsoids of porphyrin ligands (except for pyrrolic nitrogens) are omitted for clarity.

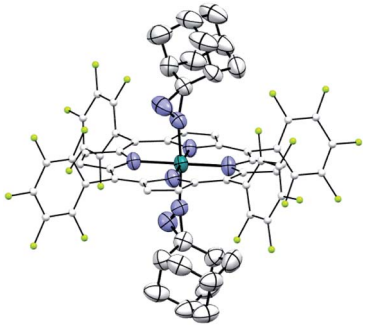

Fig. 3 ORTEP diagram of **2az** with thermal ellipsoids at the 50% probability level. Hydrogen atoms and ellipsoids of porphyrin ligands (except for pyrrolic nitrogens) are omitted for clarity.

Table 2 Carbene chemical shifts δ (ppm)[a,b]

δ(Fe=C)		δ(Ru=C)	
1a	413.57	**2a**	369.55
1b	394.92	**2b**	353.72
1a·ArNC	444.78		
1a·CNPy	433.85		
δ(Fe=C)		δ(Os=C)	
1a·Py	433.58	**3a**	351.28[c]
1a·NMe$_2$Py	433.39	**3b**	367.04[c]
1a·MeIm	433.36	**3c**	350.39

[a] Measured in $CDCl_3$ at 298 K. [b] ArNC = 2,6-dimethylphenyl isocyanide, CNPy = 4-cyanopyridine, Py = pyridine, NMe$_2$Py = 4-dimethylaminopyridine, and MeIm = 1-methylimidazole. [c] Measured in C_6D_6 at 298 K.

Spectral features

All the ^{1}H NMR signals of dialkylcarbene complexes **1–3** are in the diamagnetic region, and no significant spectral change was observed up to 60 °C under an inert atmosphere. The Ad protons of these M=Ad complexes (Scheme 1) are strongly shielded and well separated by the porphyrin ring current, as assigned by COSY spectra (see the ESI†). In the case of ^{13}C NMR spectra, the five-coordinate Fe-dialkylcarbene complexes **1** show characteristic downfield carbene chemical shifts at 394.92–413.57 ppm, and ligation of **1a** with an axial ligand such as isocyanide, imidazole, or pyridines results in further downfield shifts of carbene carbons to 433.36–444.78 ppm; less deshielded signals are observed in Ru-mono(dialkylcarbene) complexes **2** as well as Os-bis(dialkylcarbene) complexes **3** (350–370 ppm, Table 2).

Several other spectroscopic techniques were employed to probe the oxidation state of metal centers in these metalloporphyrin dialkylcarbene complexes. The Fe K-edge XANES spectrum of **1a** was recorded along with that of several reference iron porphyrin complexes. The pre-edge peak of **1a** (7113.0 eV) is highly similar to that of [Fe^{II}(TPFPP)(CPh$_2$)] (7113.0 eV) yet appreciably lower in energy than that of [Fe^{III}(TPFPP)Cl] (7114.0 eV), thus suggesting an Fe(II) center in the dialkylcarbene complex (Fig. 4, top). These results are also consistent with those obtained previously for Fe porphyrin carbene and related complexes (Table S6†).[16a] The ^{57}Fe isomer shift (δ = 0.25 mm s^{-1}) of **1a** in Mössbauer spectroscopy (Fig. 5) falls in the region of low-spin five-coordinate Fe(II) porphyrin complexes (−0.03 to 0.37 mm s^{-1});[16c] the relatively small quadrupole splitting ($|\Delta E_Q|$ = 1.61 mm s^{-1}) is possibly related to the unique ligand field induced by the dialkylcarbene ligand.[29] The resonance Raman spectrum of **1a** features a 1356 cm^{-1} band (Fig. S5†) which is comparable to that of [Fe(TPP)(CCl$_2$)] (1368 cm^{-1}) and indicative of a low spin Fe(II) center (1358–1379 cm^{-1}) rather than other higher valent configurations (>1370 cm^{-1} for Fe in +3 to +5 oxidation states).[16a,30] The diamagnetism of **1a** is also suggested by Evans' method where no observable separation of solvent peaks was found. Ruthenium complex **2b** displays an oxidation-state marker band at 1009 cm^{-1} in its IR spectrum, which is within the normal range of Ru(II) porphyrin carbonyl or carbene complexes (1001–1017 cm^{-1}).[17g,31]

Previously, the oxidation state of metal centers in Os porphyrin carbene complexes remained ambiguous.[18c,e,f] To clarify this issue, we conducted an Os L-edge XANES study on **3a** and two related Os porphyrins (Fig. 4, bottom). Complex **3a** exhibits an L$_3$-edge peak at 10 879.0 eV in its XANES spectrum, and this was found to be highly similar to that of [Os^{II}(4-F-TPP)(CO)] (10 879.0 eV) but different from that of the high-valent *trans*-dioxo complex [Os^{VI}(TTP)O$_2$] (10 880.0 eV); these results are supportive of an Os^{II}-bis(carbene) electronic structure of **3a** rather than an Os^{VI} Schrock alkylidene formulation.

UV-vis absorption spectra of Fe complexes **1a**,**b** both exhibit a single Soret band, whereas two separate Soret bands could be observed for Ru congeners (Fig. S1†). Addition of an axial ligand generally leads to a red shift of the Soret band(s), and the extent of the red shift is affected by the electronic properties of the

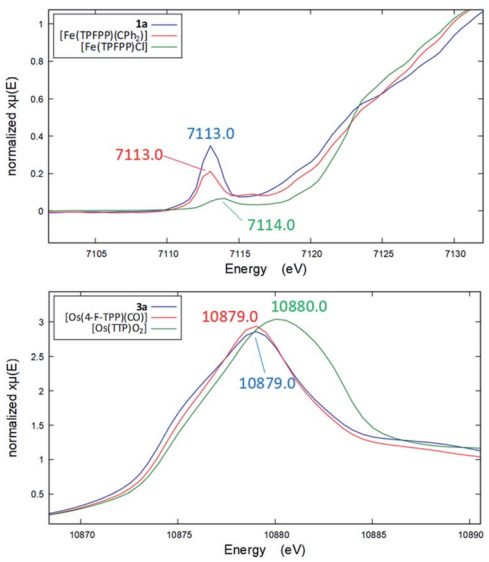

Fig. 4 Top: Fe pre-edge peaks in the XANES spectra of **1a** (blue), [Fe(TPFPP)(CPh$_2$)] (red), and [Fe(TPFPP)Cl] (green). Bottom: Os L$_3$-edge peaks in the XANES spectra of **3a** (blue), [Os(4-F-TPP)(CO)] (red), and *trans*-dioxo complex [Os(TTP)O$_2$] (green).

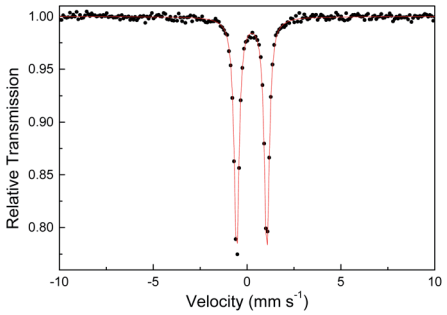

Fig. 5 Zero-field Mössbauer spectrum of **1a** at 298 K.

axial ligand (Fig. 6). The binding constants of pyridine with **1a** and **2b** were measured to be $(9.90 \pm 0.48) \times 10^2$ and $(2.375 \pm 0.144) \times 10^4$ M^{-1} respectively (Fig. S2†), both being smaller than those of analogous Fe/Ru porphyrin complexes bearing other carbene ligands (3500 M^{-1} for Fe-dichlorocarbene[11a] and 1.13×10^5 M^{-1} for Ru-quinoid carbene complexes[17f]). Interestingly, no binding between PPh_3 and **1a**/**2b** has been observed during UV-vis monitoring. The Soret and Q bands of Os-bis(-dialkylcarbene) complexes **3** are generally weakened and broadened, with the Q bands of **3b,c** markedly blue-shifted (<500 nm) as compared to those of **1a,b** and **2a,b** bearing the same porphyrin ligands (Fig. S1†); these spectral features are typically found for Os porphyrin complexes.[32]

Electrochemistry

Electrochemical studies on these group 8 metal dialkylcarbene complexes were conducted to gain insights into their electronic structures (Fig. 7 and S3†). Complexes **1a,b** both show one reversible oxidation wave at −0.18 to 0.01 V (*vs.* $Fc^{+/0}$, the same as below) in the cyclic voltammograms (Table 3), falling in the region of the $Fe^{III/II}$ couple.[33] This assignment complied with the results from XANES, Mössbauer, and resonance Raman spectroscopies (*vide supra*), and was further verified by the spectroelectrochemical spectrum of **1a** in which a broadened Soret band and red-shifted Q bands characteristic of Fe(III) porphyrins appeared after oxidation (Fig. 8, top);[34] products

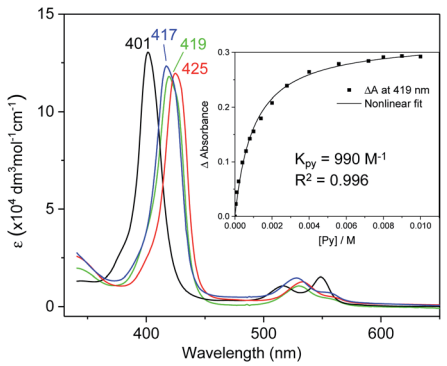

Fig. 6 UV-vis spectra of **1a** (black), and **1a** ligated with 4-cyanopyridine (blue), pyridine (green), and 4-dimethylaminopyridine (red) in DCM. Inset: titration of pyridine (5×10^{-5}–0.01 M) into a DCM solution of **1a** (5×10^{-5} M).

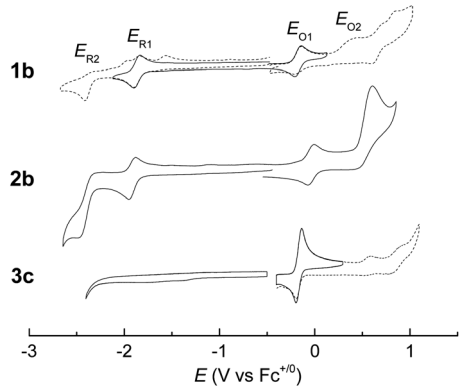

Fig. 7 Cyclic voltammograms of group 8 metal dialkylcarbene complexes supported by the TTP macrocycle, using 0.1 M $(Bu_4N)PF_6$ as the electrolyte and at a scan rate of 0.1 V s^{-1}. Top: **1b** and **2b**, measured in DMF with SCE as the reference electrode; $E(Fc^{+/0}) = 0.49$ V. Bottom: **3c**, measured in DCM with Ag/AgCl as the reference electrode; $E(Fc^{+/0}) = 0.40$ V. Dotted lines indicate irreversible redox events.

derived from porphyrin- or carbene ligand-oxidation could be precluded, since metal-$Por^{+\bullet}$ species feature a broad band between 630 and 710 nm while oxidation on the axial ligand generally leads to minor changes in the electronic spectra of [M(Por)] complexes.[33,35] Although the oxidation is reversible on the cyclic voltammetry timescale, the oxidized Fe(III) species was found unstable and decomposed within minutes. The first reversible oxidation waves of **2a,b** (−0.03 to 0.18 V, Table 3) are also ascribed to be Ru-centered oxidation according to our previous study.[17g] The Os complexes **3a–c** all show a quasi-reversible oxidation wave (−0.17 to 0.04 V) assignable to the $Os^{III/II}$ couple,[36] in agreement with the +2 oxidation state of the Os center suggested by XANES spectroscopy (Fig. 4, bottom). The second oxidation waves in **1b**, **2b**, **3a**, and **3c** could be attributed to porphyrin-centered oxidation processes. The first reduction waves of the Fe complexes are strongly influenced by the aryl substituents on porphyrin ligands (Table 3) and are therefore assigned to porphyrin-centered reduction. This was also evidenced by the noticeable spectral changes of Soret and Q bands upon reduction of **1a** (Fig. 8, bottom). The first reductions of **2a,b** and **3a,b** are assigned likewise in view of their

Table 3 Redox potentials V *vs.* $Fc^{+/0}$[a]

E (V)	E_{O1}	E_{O2}	E_{R1}	E_{R2}
1a	0.01		−1.59	−2.07
1b	−0.18	0.47[b]	−1.86	−2.38[c]
2a	0.18		−1.66	−2.10
2b	−0.03	0.61[b]	−1.91	−2.50[c]
3a	−0.10[d]	0.77[b]	−2.05[d]	
3b	0.04[d]		−1.71[d]	
3c	−0.17[d]	0.59[b]		

[a] $E_{1/2}$ values. **1a,b** and **2a,b** were measured in DMF with SCE as the reference electrode; $E(Fc^{+/0}) = 0.49$ V. **3a–c** were measured in DCM with Ag/AgCl as the reference electrode; $E(Fc^{+/0}) = 0.40$ V. [b] $E_{p,a}$. [c] $E_{p,c}$. [d] Quasi-reversible.

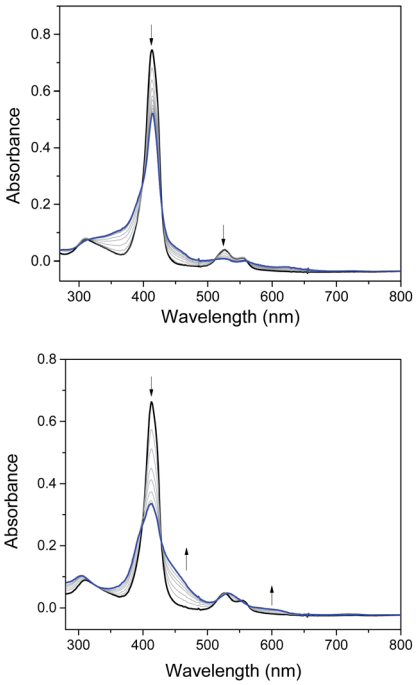

Fig. 8 Spectroelectrochemistry of **1a** in DMF. Electrode potentials: 0.6 V (top) and −1.1 V (bottom) *vs.* Ag/AgCl.

similarity in potential and reversibility (Table 3); no reduction peaks are observed for **3c** and they are possibly beyond the solvent window of DCM.

DFT calculations

DFT calculations were performed on **1b** and **3a** to provide detailed information on the bonding nature of a metalloporphyrin mono(dialkylcarbene) complex and a metal-bis(dialkylcarbene) complex. The optimized structure of **1b** and **3a** show the M–$C_{carbene}$ (M = Fe, Os) bond distances of 1.742 Å and 2.003 Å respectively, which are close to the experimental values (Table 1). A low-spin Fe(II) center with an electronic configuration of $(d_{x^2-y^2})^2(d_{yz})^2(d_{xz})^2(d_{z^2})^0(d_{xy})^0$ was found for **1b** (Fig. 9), consistent with the diamagnetism of this complex and also similar to previous experimental and computational results for iron porphyrin complexes ligated with other types of carbene ligands.[16b,37] An Fe-dialkylcarbene π-backbonding interaction is formed between the d_{yz} of Fe and the p_y orbital of $C_{carbene}$, and the π(Fe=C) orbital is mostly Fe d_π in character (H-3, 45% Fe, 17% $C_{carbene}$), while the π^*(Fe=C) orbital is more polarized to the carbene carbon (L + 2, 32% Fe, 52% $C_{carbene}$). Therefore, the complex should be best described as a formally Fe^{II}=Ad^0 species with decent Fe-to-carbene π-backbonding. Similar to free Ad in which hyperconjugation plays an essential role in stabilizing the carbene center,[22d,e] the π^*(Fe=C) he orbital in **1b** is also stabilized by such an effect exerted by the flanking alkyl groups. The LUMO is essentially populated on the porphyrin ligand and the HOMO mostly resides at the Fe center, both of which comply with the electrochemical study (*vide supra*).

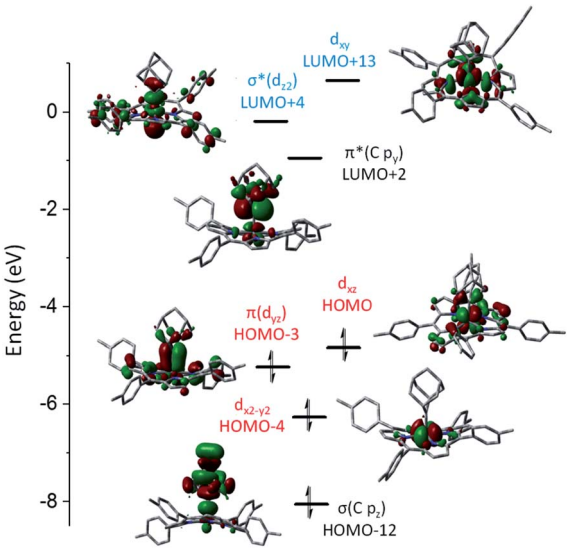

Fig. 9 Calculated molecular orbitals of [Fe(TTP)(Ad)] (**1b**). LUMO, which is mainly located on the TTP ligand, is not shown. The *z* axis is orthogonal to the porphyrin plane and the *x* and *y* axes are on the porphyrin plane and bisecting Fe–$N_{pyrrole}$ vectors.

A similar M(II) electronic configuration was calculated for Os-bis(dialkylcarbene) complex **3a** which features a low-spin d^6 Os(II) center and strong metal-carbene covalency (Fig. 10, top). The two perpendicular p_π orbitals of the two Ad ligands interact with the d_{xz} and d_{yz} orbitals of Os, giving rise to two pairs of almost degenerate π(Os=C) (H-1 and H-2) and π^*(Os=C) (L + 2 and L + 3) orbitals. Different from **1b**, the d_{z^2} orbital of **3a** is higher in energy than d_{xy} as a result of the strongly coordinating dialkylcarbene ligands. TD-DFT calculations could well reproduce the UV-vis spectrum of **3a** which consists of two separate Soret bands at 343–395 nm and a weak and broad Q band at 557 nm (Fig. 10, bottom).

Stability and reactivity

Fe(II) porphyrins are usually air-sensitive and could be stabilized by a few π-acceptor ligands (*e.g.*, CS and isocyanides). In this work, the dialkylcarbene Ad ligand was found to confer remarkable stability on Fe(II) porphyrins, especially for **1a** bearing the electron-deficient porphyrin ligand TPFPP. No decomposition of **1a** could be detected even by treating its benzene solution at 80 °C in air for at least 1 h; its six-coordinate adducts with pyridines and MeIm also stayed intact in solution for at least one week under ambient conditions, which is in sharp contrast to air-sensitive [Fe(TPFPP)(CPh_2)(MeIm)].[11e] Surprisingly, thermogravimetric analysis (TGA) revealed that **1a** in the solid state is stable up to ~230 °C in air (Fig. S6;† the ^{1}H NMR spectrum of **1a**, after being heated at 230 °C in the solid state for 5 min in air, remained unchanged). The Ru analogue **2a** also exhibits great thermal stability in air with the onset of decomposition appearing at ~330 °C (Fig. S6†). The Os-bis(dialkylcarbene) complexes are stable below 60 °C under an inert atmosphere in both solution and solid states.

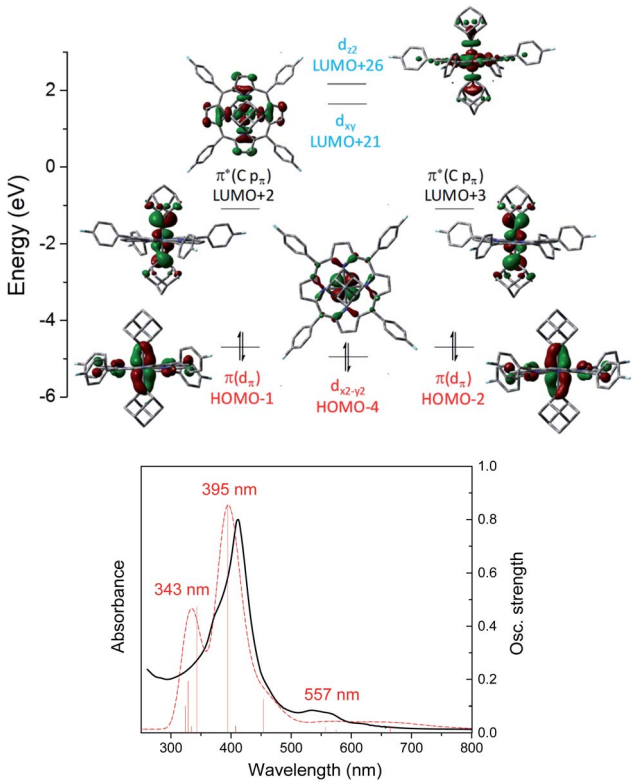

Fig. 10 Top: Calculated molecular orbitals of [Os(4-F-TPP)(Ad)$_2$] (**3a**). The *z* axis is orthogonal to the porphyrin plane and the *x* and *y* axes are on the porphyrin plane and bisecting Os–$N_{pyrrole}$ vectors. Bottom: Experimental (black solid line) and TD-DFT simulated (red dashed line) UV-vis spectrum of **3a**.

Although Fe porphyrin CPh_2 and $C(Ph)CO_2Et$ carbene complexes could react stoichiometrically with alkenes and/or $C(sp^3)$–H bonds,[11e] **1a** was found resistant toward various organic substrates/nucleophiles (*e.g.*, styrene, 1,4-cyclohexadiene, $PhNH_2$, and PPh_3; see the ESI† for details), even in the presence of a *trans* axial ligand (pyridine and MeIm) and at high temperature (80 °C), nor was it reactive under UV irradiation, which has been reported to trigger reactions between [Fe(TPP)(CX_2)] (X = halogens) and alkenes.[38] Remarkable stability was also found with the Ru congener **2a** which was unreactive under the above conditions. When **1a** was treated with anionic nucleophiles such as NaXMe (X = S, O) at 80 °C, S_NAr reactions on the TPFPP *meso*-C_6F_5 groups slowly took place to afford **1c** and **1d** respectively (reaction 9 in Scheme 2), which could be traced by the changes in ^1H and ^{19}F NMR spectra; the carbene carbons remained intact and still resonated at ~410 ppm in their ^{13}C NMR spectra, demonstrating the remarkable kinetic inertness of the Ad ligand.

Previously, the Os-bis(CPh_2) complex has been shown to display stoichiometric diarylcarbene transfer reactivity.[18e] However, no dialkylcarbene transfer product was detected when treating nucleophilic organic substrates (*e.g.*, styrene, 1,4-cyclohexadiene, $PhNH_2$, PhNO, PPh_3, and PhSH) with the bis(dialkylcarbene) complex **3a** up to 60 °C; further heating up the reaction mixture to 80 °C only caused decomposition of **3a** to complicated mixtures, which was similarly observed in a control

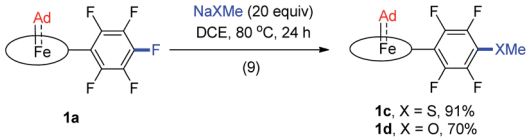

Scheme 2 Intermolecular reactions of **1a** with anionic nucleophiles.

experiment in the absence of a substrate. Surprisingly, **3a** was also stable against MeLi at −78 °C to room temperature, although MeLi was known to undergo nucleophilic addition or α-deprotonation of metal-carbene complexes. Addition of pyridine into a DCM solution of **3a** at room temperature slowly led to carbene ligand dissociation and formation of 2-adamantanone, yet neither a dialkylcarbene transfer product nor an Os-mono(dialkylcarbene) complex could be observed.[18f,g] In view of the relatively labilized Ad ligands in the Os-bis(dialkylcarbene) complexes **3**, we wondered whether **3a** would exhibit partial nucleophilic free dialkylcarbene character;[22f] however, it was found unreactive toward electrophiles such as ethyl acrylate or bis(pinacolato)diboron.

While the studies described above revealed that the dialkylcarbene Ad ligand coordinated to group 8 metal porphyrins is less reactive than diphenylcarbene CPh_2, their relative thermodynamic stability was further probed by carbene substitution experiments (Scheme 3). It was found that [Fe(TPFPP)(CPh_2)] and [Os(TPFPP)(CPh_2)$_2$] could readily react with free Ad, generated from photolysis of aziadamantane, to afford **1a** and **3b**, respectively (reactions 10 and 12 in Scheme 3), yet treatment of **1a** or **3b** with excess diazo compound Ph_2CN_2 was not able to result in replacement of the Ad ligand(s) in the Fe or Os complex by CPh_2 even under more forcing conditions (reactions 11 and 13 in Scheme 3). For the reaction of **1a** with Ph_2CN_2 (reaction 11 in Scheme 3), the azine product $Ph_2C{=}N{-}N{=}CPh_2$ was obtained in 90% yield.

Catalytic intermolecular donor–donor carbene transfer reactions catalyzed by 1a

Given the remarkable stability of the Ad ligand, we examined the possibility of using **1a** as a robust Fe(II) catalyst for some

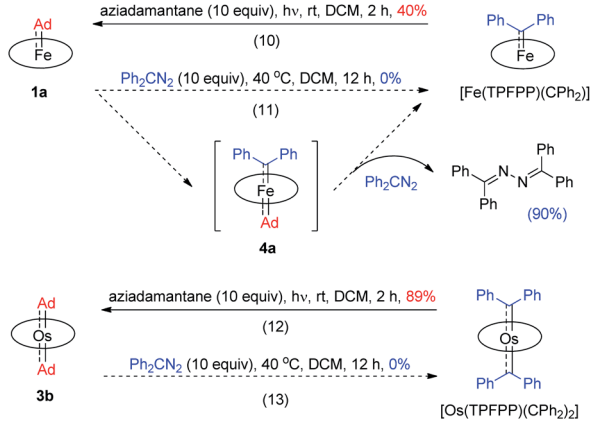

Scheme 3 Carbene substitution experiments.

challenging transformations. Diarylcarbene (CAr_2) transfer reactions remain less developed in the literature, which is mainly due to the intrinsic low reactivity of CAr_2 carbenes and they are known to form isolable adducts even with the most active catalysts such as Rh[39] and Cu.[40] Inspired by the carbene substitution experiments (reaction 11 in Scheme 3) revealing the formation of an azine product, we envisioned that **1a** might serve as an efficient catalyst for diarylcarbene transfer reactions, since the observed azine product possibly resulted from reaction of Ph_2CN_2 with a reactive Fe-bis(carbene) intermediate [Fe(TPFPP)(Ad)(CPh_2)] (**4a**, Scheme 3; by drawing an analogy with Os-bis(carbene) analogues), in which the CPh_2 ligand was activated with the *trans*-Ad ligand. Gratifyingly, cyclopropanation of styrene with Ph_2CN_2 could be catalyzed by 2 mol% of **1a** in excellent yield (90%, entry 1 in Table 4). The time course plot of this reaction showed that product **5a** was smoothly produced with a very short induction period, and catalyst **1a** remained rather stable in the reaction mixture (85% recovery, Fig. 11). Employing [Fe^{II}(TPFPP)] as the catalyst led to a poorer yield of **5a** (entry 2 in Table 4), which suggests the important role played by the Ad ligand in **1a** in this reaction. Complex **1a** showed superior catalytic performance and chemoselectivity to other commonly used carbene transfer catalysts (*e.g.*, Rh and Cu catalysts, entries 4–6 in Table 4; see also Table S7†) under the same reaction conditions since the latter catalysts afforded mainly the azine product; the Ru-dialkylcarbene complex **2a** gave slightly better results than **1a** (entry 3). By using **1a** as the catalyst, the scope of alkenes was extended to styrenes bearing electron-donating (**5b,c**) and -withdrawing (**5d**) substituents with good to high product yields (Scheme 4). A conjugated alkene was selectively cyclopropanated at the less hindered site in a moderate yield (**5e**). However, alkyl-substituted alkenes such as 1-octene resulted in a low yield of **5f** and mainly the azine by-product. Besides CPh_2 carbene, electron-deficient (**5g**) and -rich (**5h,i**) diarylcarbenes were also converted to the desired cyclopropanes in high yields.

Complex **1a** could also catalyze intermolecular S–H, N–H, and O–H insertion reactions, thereby introducing benzhydryl groups onto various heteroatoms (Scheme 4). S–H bonds activated by aryl (**6a–c**) and 2-pyridyl groups (**6d**) readily underwent carbene insertion in 88–99% yields; alkyl-substituted thiols such as ethanethiol also afforded the desired sulfide product albeit in a lower yield (**6e**, 33%). Catalytic N–H insertion could be achieved in high yields by using electron-rich N-heterocycles such as carbazole (**7a**) and imidazole (**7b**), as well as secondary alkyl amines such as morpholine (**7c**); primary amines, aryl (**7d**) and aliphatic (**7e**), resulted in only moderate product yields. Aryl alcohols including phenols (**8a,b**) and 2-naphthol (**8d**) were transformed into O–H insertion products in 75–92% yields, yet electron-poor phenol (**8c**) and aliphatic alcohol (**8e**) showed appreciably lower reactivity. Notably, catalytic C(sp^3)–H insertion of CPh_2 carbene was achieved under more demanding conditions (80 °C and dropwise addition of Ph_2CN_2), and previously such catalytic transformations were largely confined to intramolecular versions using Rh catalysts.[41] C–H insertion of doubly-activated substrates including 1,4-cyclohexadiene (**9a**) and fluorene (**9b**) was achieved in moderate yields, while a low yield was observed with the less reactive indane (**9c**). Moreover, the robustness of catalyst **1a** could be demonstrated by the high recovery of **1a** after most of the catalytic reactions mentioned above (Scheme 4).

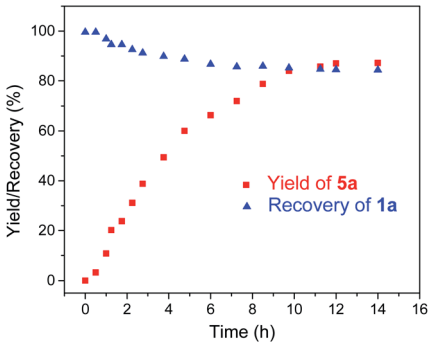

Fig. 11 Time course plot of the reaction among Ph_2CN_2, styrene, and **1a** during ^{1}H NMR monitoring.

Attempts to isolate or directly detect the proposed Fe-bis(carbene) intermediate **4a** have not been successful. We performed DFT calculations on a model complex **4b** (Fig. 12), which is identical to **4a** except that the *meso*-aryl groups in **4a** were replaced by hydrogen for simplicity.[37,42] The calculated structure of **4b** features a rather lengthened Fe–C_{CPh_2} bond (1.96 Å) as compared to the Fe–C_{Ad} bond (1.89 Å); the LUMO was mainly localized on the p_π of C_{CPh_2} while the p_π of C_{Ad} was higher in energy (L + 3); this could account for the relatively high reactivity of CAr_2 ligands as well as the stability of **1a** and its Ad ligand during catalytic turnover.

Catalytic intermolecular cyclopropanation reactions of other donor–donor (phenyl/alkyl- and dialkyl-) carbenes were also tested by using freshly prepared or *in situ* generated diazo compounds.[43] Complex **1a** could catalyze the reactions of $N_2C(Ph)CF_3$ and $N_2C(Ph)Me$ (the latter was generated *in situ* from acetophenone hydrazone and Ag_2O) with styrene to afford the corresponding cyclopropanation products in moderate to good yields albeit with low diastereomeric ratios (entries 1–2 in Table 5); however, a similar treatment of diazoadamantane (*in situ* generated from $AdNNH_2$ and PhIO) with styrene using catalyst **1a** did not give the cyclopropanation product, and [3 + 2]

Table 4 Comparison of catalytic performance among **1a**, **2a**, and other common carbene transfer catalysts[a]

Entry	Catalyst	Yield of **5a**[b] (%)
1	**1a**	90
2	[Fe^{II}(TPFPP)]	48
3	**2a**	92
4	[$Rh_2(esp)_2$]	10
5	CuI	1
6	[Ru(TTP)(CO)]	56

[a] Conditions: Ph_2CN_2 (0.2 mmol), styrene (2 mmol), catalyst (0.004 mmol), DCM (1 mL), 40 °C, 12 h, and under Ar. [b] Yield determined by ^{1}H NMR with PhTMS as the internal standard.

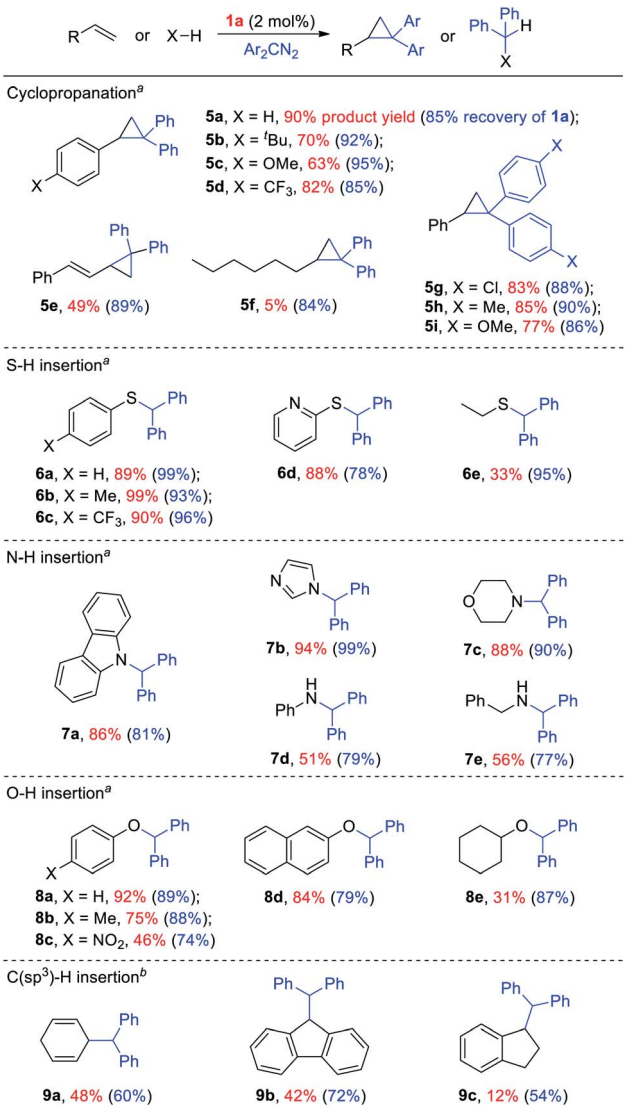

Scheme 4 Intermolecular diarylcarbene transfer reactions catalyzed by **1a**. Product yields in red and recovery of **1a** (blue) in parentheses. [a] Conditions: Ph_2CN_2 (0.2 mmol), substrate (2 mmol), catalyst (0.004 mmol), DCM (1 mL), 40 °C, 12 h, and under Ar. [b] Conditions: Ph_2CN_2 (0.2 mmol, added over 3 h), substrate (2 mmol), catalyst (0.004 mmol), DCE (1 mL), 80 °C, 12 h, and under Ar.

cycloaddition between styrene and the diazo compound to give **10** was the major reaction observed (entry 3 in Table 5).[43c] Worthy of note is the high recovery of **1a** in all these reactions as this complex showed decent stability toward PhIO which is known to generate Fe-oxo species with common Fe porphyrin complexes.[44]

Discussion

Middle/late transition metal (TM) (di)alkylcarbene species are key intermediates related to olefin metathesis[5] and (di)alkylcarbene transfer catalysis,[13,45] yet the electronic properties of dialkylcarbene as a ligand, especially in comparison with common carbene ligands including "stable" (NHC and CAAC) and "reactive" (phenyl-/ester-substituted) carbenes, still remain

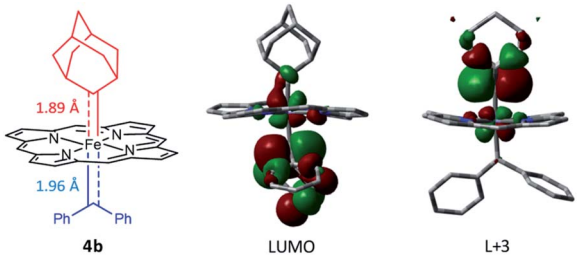

Fig. 12 DFT-optimized structure of model complex **4b** (left) and its LUMO (middle) and L + 3 orbitals (right).

less understood. In this work, by choosing 2-adamantylidene (Ad) as a rigid model, we have synthesized several terminal group 8 metal dialkylcarbene complexes from easily accessible precursors and by a simple and mild method. We have also demonstrated that, different from the well documented reactive features, dialkylcarbene ligands such as Ad can be highly stable upon coordination to TMs including Fe and even act as a robust ancillary ligand for catalytic applications. To gain deeper knowledge, the following aspects of the dialkylcarbene ligand Ad coordinated to TMs are discussed in this section.

Dialkylcarbene *vs.* common carbene ligands

Although both stable and reactive carbene ligands feature an sp^2-hybridized carbene center with a vacant p_π orbital, they have scarcely been linked or discussed together due to the drastic differences in the molecular structure, stability, and/or electronic properties of their metal complexes.[46] The uniqueness of dialkylcarbene lies in the fact that it possesses mutual characters from the above two types of carbenes: on the one hand, its carbene transfer reactivity has been well documented in the literature;[10,13,45] on the other hand, we have discovered in this work that it confers remarkable thermodynamic and kinetic stability on group 8 metal porphyrin complexes and in particular, it leads to stabilization of an Fe(II) porphyrin species and several Os-bis(-carbene) complexes. These findings prompt us to make a closer comparison between dialkylcarbene and stable/reactive carbenes with the aid of theoretical calculations.

(i) Dialkylcarbene *vs.* stable carbenes (NHC/CAAC). The carbene substituents for dialkylcarbene and stable carbenes show an interesting pattern ranging from diamino (NHC), amino/alkyl (CAAC) to dialkyl (Ad), and such a variation can directly influence their carbene frontier orbitals, *i.e.*, the σ orbital and p_π orbital, through inductive and mesomeric effects.[47] By performing DFT calculations on these free carbenes, we found that the most striking feature of dialkylcarbene is its much lower-lying p_π orbital than NHC and CAAC ($\Delta E > 1.8$ eV, Fig. 13a), likely due to the absence of π-donating atoms adjacent to the carbene center;[48] its σ orbital is also slightly higher in energy ($\Delta E = 0.10$–0.52 eV). Therefore, dialkylcarbene acts as a much stronger π-acceptor and a slightly better σ-donor, and thus a stronger-field ligand than these conventional stable carbenes.

The variation in π-character could account for the distinct differences in the Fe/Ru–$C_{carbene}$ distances, as the Fe/Ru–C_{Ad}

Table 5 Intermolecular cyclopropanation reactions between other diazo compounds and styrene catalyzed by **1a**[a]

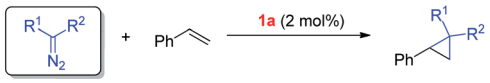

(In situ generated) diazo compound

Entry	Diazo compound	Yield of cyclopropane[b] (dr)	By-product	Recovery of **1a**
1		71% (2.4 : 1)		90%
2[c]		45% (2.0 : 1)	Azine	88%
3[d]		0%	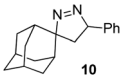 10	81%

[a] See the ESI for detailed reaction conditions. [b] Yield and diastereomeric ratio (dr) determined by ^{1}H NMR with PhTMS as the internal standard. [c] *In situ* generated diazo compound from acetophenone hydrazone and Ag_2O. [d] *In situ* generated diazo compound from 2-adamantanone hydrazone and PhIO.

bonds are all within double bond regions (Table 1) and are apparently shorter than those in NHC/CAAC complexes (1.87–2.15 Å for Fe and 1.93–2.15 Å for Ru).[49] The redox potential of metalloporphyrin carbene complexes, especially the first oxidation potential (E_{O1}), is a good indicator for the electronic properties of carbene ligands,[17l] and the greater π-acidity of the Ad ligand is also noted by the increased E_{O1} values of **2a,b** as compared to their NHC congeners (Fig. 14 and Table S8†). In addition, NHC often gives bis(carbene) complexes with Fe and Ru porphyrins,[49d,j] yet only mono(dialkylcarbene) complexes of Fe and Ru porphyrins [$M_{Fe/Ru}$(Por)(Ad)] are isolable, which is likely caused by the prominent *trans* influence of the Ad ligand. The stronger *trans* influence of Ad than NHC is also inferred by comparing the solid-state structures of [Ru(TTP)(Ad)(MeOH)] (**2b**·MeOH) and [Ru(TPP)(IMe_2)(THF)] where the axial Ru–O bond is longer in the former (2.36 Å) than in the latter complex (2.22 Å, Fig. S7†).

(ii) Dialkylcarbene *vs.* reactive carbenes (phenyl-/ester-substituted carbenes). Besides all being related to carbene transfer catalysis, dialkylcarbene also bears some other resemblance to reactive carbenes. For instance, their complexes of Fe/Ru porphyrins are all mono(carbene) species diaplaying M–$C_{carbene}$ double bond character (1.77–1.83 Å for Fe and 1.81–1.88 Å for Ru);[16a,17g,i] these complexes share similar features in their NMR, UV-vis, and IR spectra and cyclic voltammograms. To further compare their electronic properties, we conducted DFT

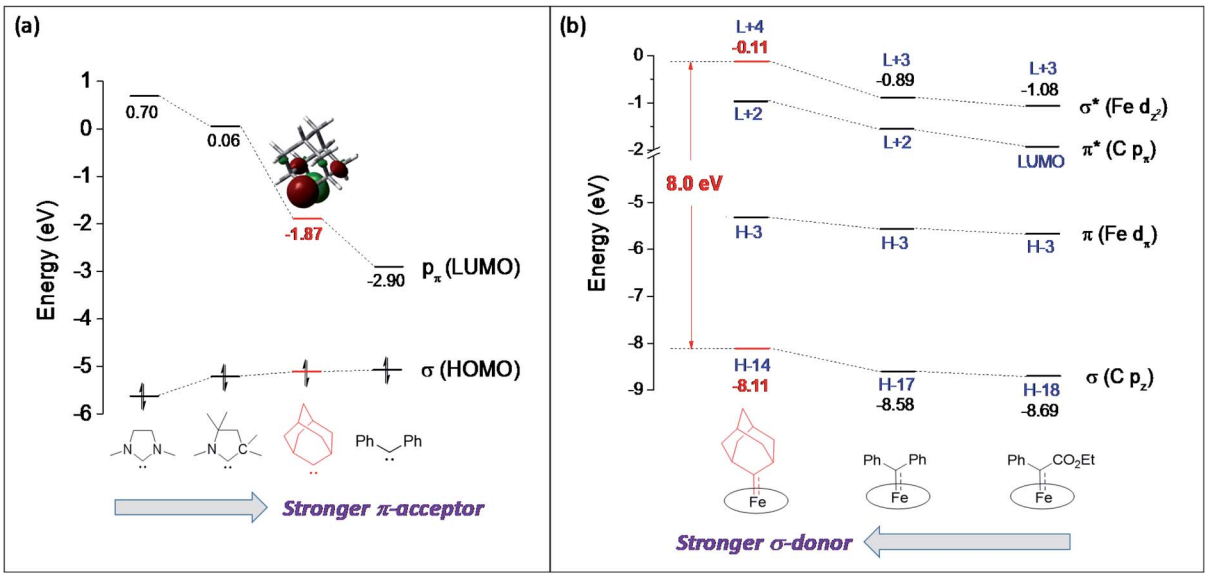

Fig. 13 (a) Comparison of calculated carbene frontier orbitals of free NHC, CAAC, Ad, and CPh_2 carbenes in their singlet states. (b) Comparison of calculated Fe–$C_{carbene}$ orbitals in [Fe(Por)(Ad)], [Fe(Por)(CPh_2)], and [Fe(Por)($C(Ph)CO_2Et$)].

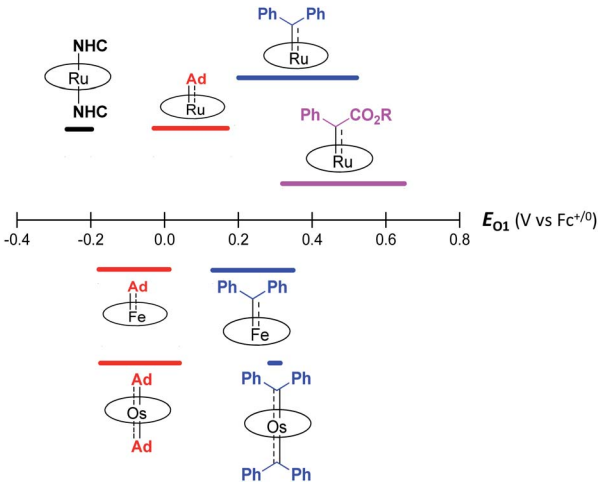

Fig. 14 First oxidation potential (E_{O1}) range of group 8 metal porphyrin carbene complexes.

calculations on Fe-carbene complexes bearing Ad, CPh_2, and $C(Ph)CO_2Et$ ligands since they have all been isolated in this work or in a previous report;[11e] the porphyrin *meso*-substituents are again replaced by hydrogen atoms for simplicity. The most notable difference between dialkylcarbene Ad and reactive carbenes lies in the σ-properties, as the Fe d_{z^2} orbital in the Ad complex is calculated at a much higher energy level ($\Delta E \geq 0.78$ eV) together with a relatively large energy splitting between σ and σ* orbitals (Fig. 13b), which is attributable to the electron-donating alkyl substituents. Meanwhile, its Fe d_π orbital is also slightly destabilized compared to that of CPh_2 and $C(Ph)CO_2Et$ carbene complexes (ΔE = 0.25–0.35 eV). Therefore, dialkylcarbene Ad is a stronger σ-donor and slightly weaker π-acceptor, and thus a more electron-donating ligand than the other reactive carbenes.

These computational results are supported by a number of spectroscopic and experimental data. The electron-donating feature of dialkylcarbene can be demonstrated by electrochemical studies where the E_{O1} values of Ad complexes of group 8 metal porphyrins are appreciably smaller than those of phenyl-/ester-substituted carbene congeners (Table 6 and Fig. 14);[17g] additionally, a larger isomer shift in the Mössbauer spectrum of **1a** (0.25 mm s^{-1}) than that of the analogous CPh_2 (0.03–0.19 mm s^{-1}) and CCl_2 complexes (0.02–0.10 mm s^{-1}) also reveals a more electron-rich Fe center in the former complex. The much enhanced σ-bonding interaction improves the *trans* influence, as revealed by smaller binding constants of **1a** and **2b** (see the Results section), as well as the thermodynamic stability of dialkylcarbene Ad relative to other reactive carbene complexes, which has been demonstrated by the carbene substitution experiments (Scheme 3). The higher carbene p_π orbital in dialkylcarbene complexes is accountable for the kinetic stability of **1a** and **3a** since they were observed to be unreactive towards stoichiometric carbene transfer reactions while the analogous CPh_2 and/or $C(Ph)CO_2R$ carbene complexes have been reported to be reactive.[11e,18e]

Table 6 First oxidation potentials (E_{O1}, V *vs.* $Fc^{+/0}$) of group 8 metal carbene complexes supported by the TPFPP macrocycle

Complex	E_{O1}[a] (V)	Ref.[b]
Fe-mono(carbene) complexes		
[Fe(TPFPP)(Ad)] (**1a**)	0.01	TW
[Fe(TPFPP)(CPh_2)]	0.35	17*g*
Ru-mono(carbene) complexes		
[Ru(TPFPP)(Ad)] (**2a**)	0.18	TW
[Ru(TPFPP)(CPh_2)]	0.46	17*g*
[Ru(TPFPP)(C(Ph)CO_2Me)(MeOH)]	0.65	17*g*
Os-bis(carbene) complexes		
[Os(TPFPP)$(Ad)_2$] (**3b**)	0.04[c]	TW
[Os(TPFPP)$(CPh_2)_2$]	0.30	TW

[a] $E_{1/2}$ values of reversible oxidation processes. [b] TW = this work. [c] Quasi-reversible.

Ad *vs.* other dialkylcarbene ligands

In this work, Ad is used as a model to study the features of dialkylcarbene ligands. To examine the effect of alkyl substituents of dialkylcarbene on the frontier orbitals of the carbene carbon, we performed DFT calculations on two *in silico* complexes [Fe(Por)(CMe_2)] and [Fe(Por)(C^iPr_2)]; the two calculated complexes show almost identical Fe-carbene bonding structures to the Ad complex (Fig. S8†). However, M=Ad

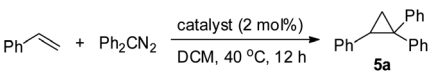

complexes (especially the Fe and Ru complexes) are uniquely stable as compared to other examples of Fe/Ru-dialkylcarbene complexes which could undergo a 1,2-hydride/alkyl shift and/or carbene transfer reaction.[7e,h,10,19b,20b,50] Such a striking difference is attributable to the rigid structure of Ad. On the one hand, its diamondoid skeleton suppresses the inner-sphere 1,2-hydride shift both thermodynamically and kinetically (Fig. 15a).[22c] On the other hand, the angle at carbene carbon is relatively fixed in Ad complexes while it is more flexible in other dialkylcarbene such as CMe_2, as revealed by DFT calculations (Fig. 15b). Such an angle is closely related to the reactivity of carbene species[47] as the energy level of the CMe_2 p_π orbital decreases significantly upon increasing this angle (Fig. S9†); in contrast, the Ad complex stays preferentially around the local minimum of its potential energy curve which is apparently steeper than that of the CMe_2 complex, thus making it less susceptible to outer-sphere nucleophilic attack.

Ad *vs.* π-acceptor ligands for Fe(II) porphyrins

Some useful comparisons can also be made among dialkylcarbene Ad and common π-acceptor ligands which are important in stabilizing Fe(II) porphyrins.[16b] While Ad only forms mono-adducts with the Fe center, bis-adducts of NO,[51] CO,[52] pyridine,[34b] and isocyanide[53] have all been reported, which implies a stronger ligand field of Ad than other π-acids. Electrochemistry revealed larger E_{O1} values for CS and NO complexes (≥0.6 V *vs.* SCE)[33,51,54] than the Ad counterparts (0.29–0.50 V *vs.* SCE) and thus suggested less electron-donating

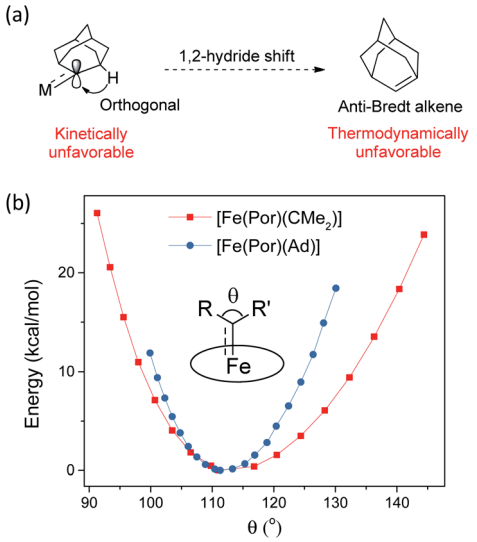

Fig. 15 (a) Resistance of M=Ad complexes toward 1,2-hydride shift. (b) Calculated potential energy curves for [Fe(Por)(Ad)] and [Fe(Por)(CMe_2)] by changing the angle θ.

properties of the diatomic ligands; this is consistent with the larger isomer shift of **1a** (0.25 mm s^{-1}) in Mössbauer spectroscopy as compared to CS and CO complexes measured at similar temperatures (−0.03 to 0.18 mm s^{-1}).[16c]

Catalytic diarylcarbene transfer reactivity

Previously, intermolecular diarylcarbene transfer reactions have only been achieved by a limited number of catalytic systems and some of them suffered from a low yield, narrow substrate scope, and/or high catalyst loading.[18e,55] The Fe-dialkylcarbene complex **1a** is, to the best of our knowledge, the first Fe catalyst that mediates the transfer of diarylcarbene to a panel of substrates with moderate to high yields, while remaining largely intact during turnover. Based on a few reports on the stoichiometric reactivity of Fe-diarylcarbene species with organic substrates,[11e,f,h] we envision that the plausible intermediates, [Fe(TPFPP)(Ad)(CAr_2)], are key to the success in our methodology and thus merit further discussion.

We have not been able to detect the presence of [Fe(TPFPP)(Ad)(CPh_2)] species. Nonetheless, according to our calculated structure of **4b** (Fig. 12), the CPh_2 carbene group is rather labile as indicated by the elongated Fe–C_{CPh_2} bond (1.96 Å), which is also consistent with the high reactivity of **1a** involving **4a** as a proposed reactive intermediate; meanwhile the Fe–C_{Ad} bond is appreciably shorter (1.89 Å) and could account for the stability of the catalyst. However, such a large difference in Fe-carbene distances is in contrast to those found in the corresponding five- or six-coordinate mono(carbene) complexes, *i.e.*, [Fe(Por)(CPh_2)] *vs.* [Fe(Por)(Ad)] or [Fe(Por)(CPh_2)(L)] *vs.* [Fe(Por)(Ad)(L)],[11e,16a,c] where both pairs of complexes display negligible differences in the Fe–carbene bond distances (<0.02 Å). We attribute this phenomenon to both the *trans* effect of Ad and the steric effect of CPh_2 carbene ligands. The steric repulsion between the bulky CPh_2 group and porphyrin ligand has been well documented in the literature, especially in six-coordinate complexes where a strong distortion of the porphyrin ligand has been observed,[11e] which is distinctly different from the nearly planar porphyrins found in six-coordinate Ad and CCl_2 carbene complexes.[11a] In previous examples with imidazoles as *trans*-axial ligands, the strong *trans* effect of CPh_2 carbene and the highly distorted porphyrin plane significantly weaken the Fe–imidazole interaction.[16c] In model complex **4b**, however, where the ligand field of Ad is comparable to that of CPh_2, the Ad group tends to stay closer to the Fe center and reduces the distortion of porphyrin toward itself; consequently, the steric effect (or Pauli repulsion) between porphyrin and CPh_2 is expected to increase, as the distance between them is as short as 2.4 Å (Fig. 16a), which is well within the normal region for π–π interaction,[56] and the electrostatic repulsion is also enhanced since both CPh_2 and porphyrin carry partial negative charge (Fig. 16b). Elongation of the Fe–C_{CPh_2} bond thus occurs in order to offset these repulsive interactions. It should be noted that such a steric effect is unique to metalloporphyrin systems, since in other common catalysts, such as Rh and Cu catalysts, the coordination environment around CAr_2 is much less congested and the aryl ring(s) on CAr_2 can even be coplanar with the carbene plane according to their crystal structures.[39,40]

Besides being spatially accessible due to the elongated Fe-carbene distance, CPh_2 carbene is also energetically favorable to be transferred to organic substrates in the bis(carbene) intermediate. While the carbene p_π orbitals of CPh_2 and Ad ligands in their mono(carbene) porphyrin complexes are both calculated at L + 2 (Fig. 13b), in the bis(carbene) complex **4b** the p_π orbital of CPh_2 is markedly lowered to the LUMO while that of Ad slightly increases to L + 3 (Fig. 12). This is likely caused by the intrinsic π-characters of the two carbene ligands as the p_π orbital of free Ad lies higher in energy than that of CPh_2 (in their singlet states) due to the hyperconjugation effect (Fig. 13a), yet the presence of two π-acceptor ligands on the Fe center decreases the metal-to-carbene backbonding and makes the carbene orbital of CPh_2 shift to a lower energy level. Meanwhile, the σ orbital of CPh_2 is also strongly destabilized, as it is mainly located at H-17 in the mono(carbene) complex (Fig. 13b), yet in **4b** it exists at H-5 and even partially at the HOMO (Fig. S10†). To briefly summarize, the elongated Fe–C_{CPh_2} bond as well as reorganized CPh_2 carbene frontier orbitals concomitantly lead to great destabilization of the CPh_2 group in the putative bis(-carbene) [Fe(Por)(Ad)(CPh_2)] intermediate, which could in turn

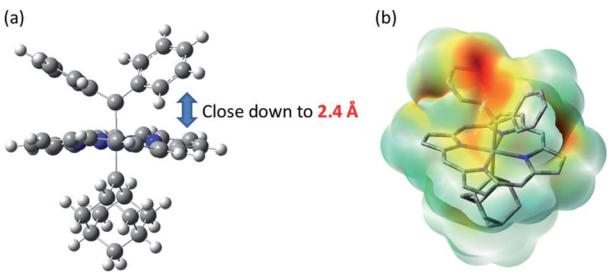

Fig. 16 (a) Spatial separaton between CPh_2 and Por ligands in the optimized structure of **4b**. (b) Calculated electrostatic map of **4b**.

account for the high catalytic activity of **1a** in these diarylcarbene transfer reactions.

Conclusions

In this work we have conducted a detailed study on a series of group 8 metal porphyrin dialkylcarbene complexes. With aziadamantane as the carbene source, a new synthetic method is developed toward Fe- and Ru-mono(dialkylcarbene) complexes and also Os-bis(dialkylcarbene) complexes, which, to the best of our knowledge, represent the first examples of transition metal-bis(dialkylcarbene) complexes. Spectroscopic investigations including XANES, NMR, electrochemistry, UV-vis, Mössbauer, resonance Raman, and IR, combined with DFT and TD-DFT calculations, reveal that the electronic structures of these dialkylcarbene complexes are all low-valent d^6 metal-carbene M^{II}=Ad^0 in nature instead of the high-valent Schrock alkylidene formalism. These dialkylcarbene complexes generally exhibit much improved thermodynamic and kinetic stability than other analogous group 8 metal porphyrins bearing nonheteroatom-stabilized carbene ligands such as diphenylcarbene; further comparison with other types of carbene ligands shows that dialkylcarbene Ad is a borderline species in between the common "stable" and "reactive" carbenes and it displays strong σ-donating as well as π-accepting characters. The unique electronic properties and stable features make dialkylcarbene Ad a promising candidate for ligand design in organometallic catalysis, and it has been demonstrated in this work that the Fe(II) complex **1a** is highly active and robust in some donor–donor carbene, especially diarylcarbene, transfer reactions where the strong-field *trans*-Ad ligand is believed to play a crucial role in activating the reactive carbene groups.

Conflicts of interest

There are no conflicts to declare.

Acknowledgements

This work is supported by the Hong Kong Research Grants Council (HKU 17303815) and Basic Research Program-Shenzhen Fund (JCYJ20170412140251576, JCYJ20170818141858021, and JCYJ20180508162429786). We thank Prof. Ya-Wen Zhang, Mr Haozong Xue, and staff at the Shanghai Synchrotron Radiation Facility (SSRF) for assistance with XANES spectroscopy, Mr Qian Liu from shiyanjia lab (https://www.shiyanjia.com) for support in Mössbauer analysis, and Prof. David L. Phillips, Dr Lili Du, Dr Zhiping Yan, and Ms Xueqin Bai for performing the resonance Raman measurements. We acknowledge helpful discussions with Prof. Michael P. Doyle and Dr Ka-Pan Shing. Assistance in experimental work by Ms Linda Quach and Ms Shuo Xu is also kindly acknowledged.

Notes and references

1 R. R. Schrock, *J. Am. Chem. Soc.*, 1974, **96**, 6796–6797.
2 R. R. Schrock, *Chem. Rev.*, 2002, **102**, 145–180.
3 (*a*) J. D. Fellmann, G. A. Rupprecht, C. D. Wood and R. R. Schrock, *J. Am. Chem. Soc.*, 1978, **100**, 5964–5966; (*b*) M. R. Churchill and W. J. Youngs, *Inorg. Chem.*, 1979, **18**, 1930–1935; (*c*) J. D. Fellmann, R. R. Schrock and G. A. Rupprecht, *J. Am. Chem. Soc.*, 1981, **103**, 5752–5758; (*d*) A. M. LaPointe, R. R. Schrock and W. M. Davis, *J. Am. Chem. Soc.*, 1995, **117**, 4802–4813; (*e*) J. B. Diminnie, H. D. Hall and Z. Xue, *Chem. Commun.*, 1996, 2383–2384; (*f*) T. Chen, Z. Wu, L. Li, K. R. Sorasaenee, J. B. Diminnie, H. Pan, I. A. Guzei, A. L. Rheingold and Z. Xue, *J. Am. Chem. Soc.*, 1998, **120**, 13519–13520; (*g*) T. Chen, X.-H. Zhang, C. Wang, S. Chen, Z. Wu, L. Li, K. R. Sorasaenee, J. B. Diminnie, H. Pan, I. A. Guzei, A. L. Rheingold, Y.-D. Wu and Z.-L. Xue, *Organometallics*, 2005, **24**, 1214–1224; (*h*) U. J. Kilgore, J. Tomaszewski, H. Fan, J. C. Huffman and D. J. Mindiola, *Organometallics*, 2007, **26**, 6132–6138; (*i*) Z.-L. Xue and L. A. Morton, *J. Organomet. Chem.*, 2011, **696**, 3924–3934.
4 For a review on Fischer-type multicarbene complexes, see: D. I. Bezuidenhout, S. Lotz, D. C. Liles and B. van der Westhuizen, *Coord. Chem. Rev.*, 2012, **256**, 479–524.
5 G. C. Vougioukalakis and R. H. Grubbs, *Chem. Rev.*, 2010, **110**, 1746–1787.
6 (*a*) W. Petz, *Iron-Carbene Complexes*, Springer-Verlag, 1993; (*b*) O. Daugulis, A. H. R. MacArthur, F. C. Rix and J. L. Templeton, *ACS Catal.*, 2016, **6**, 1518–1532.
7 (*a*) J. P. Collman, P. J. Brothers, L. McElwee-White, E. Rose and L. J. Wright, *J. Am. Chem. Soc.*, 1985, **107**, 4570–4571; (*b*) D. G. Gusev, T. Maxwell, F. M. Dolgushin, M. Lyssenko and A. J. Lough, *Organometallics*, 2002, **21**, 1095–1100; (*c*) P. Alvarez, E. Lastra, J. Gimeno, M. Bassetti and L. R. Falvello, *J. Am. Chem. Soc.*, 2003, **125**, 2386–2387; (*d*) M. Leutzsch, L. M. Wolf, P. Gupta, M. Fuchs, W. Thiel, C. Farès and A. Fürstner, *Angew. Chem., Int. Ed.*, 2015, **54**, 12431–12436; (*e*) A. Guthertz, M. Leutzsch, L. M. Wolf, P. Gupta, S. M. Rummelt, R. Goddard, C. Farès, W. Thiel and A. Fürstner, *J. Am. Chem. Soc.*, 2018, **140**, 3156–3169; (*f*) A. Fürstner, *J. Am. Chem. Soc.*, 2019, **141**, 11–24; (*g*) T. Biberger, C. P. Gordon, M. Leutzsch, S. Peil, A. Guthertz, C. Copéret and A. Fürstner, *Angew. Chem., Int. Ed.*, 2019, **58**, 8845–8850; (*h*) S. Peil, A. Guthertz, T. Biberger and A. Fürstner, *Angew. Chem., Int. Ed.*, 2019, **58**, 8851–8856.
8 (*a*) G. Ferrando, J. N. Coalter III, H. Gérard, D. Huang, O. Eisenstein and K. G. Caulton, *New J. Chem.*, 2003, **27**, 1451–1462; (*b*) M. A. Esteruelas, A. M. López and M. Oliván, *Coord. Chem. Rev.*, 2007, **251**, 795–840; (*c*) V. Martin and S. Blakey, *Tetrahedron Lett.*, 2008, **49**, 6800–6803; (*d*) T. Bolaño, M. A. Esteruelas and E. Oñate, *J. Organomet. Chem.*, 2011, **696**, 3911–3923.
9 (*a*) M. Brookhart, J. R. Tucker and G. R. Husk, *J. Am. Chem. Soc.*, 1981, **103**, 979–981; (*b*) K. A. M. Kremer, P. Helquist and R. C. Kerber, *J. Am. Chem. Soc.*, 1981, **103**, 1862–1864; (*c*) M. Brookhart, J. R. Tucker and G. R. Husk, *J. Am. Chem. Soc.*, 1983, **105**, 258–264; (*d*) M. Brookhart, D. Timmers, J. R. Tucker, G. D. Williams, G. R. Husk, H. Brunner and B. Hammer, *J. Am. Chem. Soc.*, 1983, **105**, 6721–6723; (*e*)

M. Brookhart, W. B. Studabaker and G. R. Husk, *Organometallics*, 1985, **4**, 943–944; (*f*) M. Brookhart, W. B. Studabaker and G. R. Husk, *Organometallics*, 1987, **6**, 1141–1145; (*g*) M. Brookhart, Y. Liu, E. W. Goldman, D. A. Timmers and G. D. Williams, *J. Am. Chem. Soc.*, 1991, **113**, 927–939; (*h*) E. Scharrer and M. Brookhart, *J. Organomet. Chem.*, 1995, **497**, 61–71; (*i*) S. Ishii, S. Zhao and P. Helquist, *J. Am. Chem. Soc.*, 2000, **122**, 5897–5898.

10 (*a*) K. A. M. Kremer, G.-H. Kuo, E. J. O'Connor, P. Helquist and R. C. Kerber, *J. Am. Chem. Soc.*, 1982, **104**, 6119–6121; (*b*) C. P. Casey, W. H. Miles, H. Tukada and J. M. O'Connor, *J. Am. Chem. Soc.*, 1982, **104**, 3761–3762; (*c*) C. P. Casey, W. H. Miles and H. Tukada, *J. Am. Chem. Soc.*, 1985, **107**, 2924–2931.

11 (*a*) D. Mansuy, M. Lange, J. C. Chottard, J. F. Bartoli, B. Chevrier and R. Weiss, *Angew. Chem., Int. Ed.*, 1978, **17**, 781–782; (*b*) D. Mansuy, *Pure Appl. Chem.*, 1980, **52**, 681–690; (*c*) A. Klose, E. Solari, C. Floriani, N. Re, A. Chiesi-Villa and C. Rizzoli, *Chem. Commun.*, 1997, 2297–2298; (*d*) V. Esposito, E. Solari, C. Floriani, N. Re, C. Rizzoli and A. Chiesi-Villa, *Inorg. Chem.*, 2000, **39**, 2604–2613; (*e*) Y. Li, J.-S. Huang, Z.-Y. Zhou, C.-M. Che and X.-Z. You, *J. Am. Chem. Soc.*, 2002, **124**, 13185–13193; (*f*) S. K. Russell, J. M. Hoyt, S. C. Bart, C. Milsmann, S. C. E. Stieber, S. P. Semproni, S. DeBeer and P. J. Chirik, *Chem. Sci.*, 2014, **5**, 1168–1174; (*g*) B. M. Lindley, A. Swidan, E. B. Lobkovsky, P. T. Wolczanski, M. Adelhardt, J. Sutter and K. Meyer, *Chem. Sci.*, 2015, **6**, 4730–4736; (*h*) J. Liu, L. Hu, L. Wang, H. Chen and L. Deng, *J. Am. Chem. Soc.*, 2017, **139**, 3876–3888; (*i*) J. F. DeJesus and D. M. Jenkins, *Chem.–Eur. J.*, 2019, DOI: 10.1002/chem.201905360.

12 (*a*) H. Renata, Z. J. Wang and F. H. Arnold, *Angew. Chem., Int. Ed.*, 2015, **54**, 3351–3367; (*b*) R. D. Lewis, M. Garcia-Borras, M. J. Chalkley, A. R. Buller, K. N. Houk, S. B. J. Kan and F. H. Arnold, *Proc. Natl. Acad. Sci. U. S. A.*, 2018, **115**, 7308–7313; (*c*) T. Hayashi, M. Tinzl, T. Mori, U. Krengel, J. Proppe, J. Soetbeer, D. Klose, G. Jeschke, M. Reiher and D. Hilvert, *Nat. Catal.*, 2018, **1**, 578–584.

13 (*a*) A. R. Reddy, C.-Y. Zhou, Z. Guo, J. Wei and C.-M. Che, *Angew. Chem., Int. Ed.*, 2014, **53**, 14175–14180; (*b*) A. R. Reddy, F. Hao, K. Wu, C.-Y. Zhou and C.-M. Che, *Angew. Chem., Int. Ed.*, 2016, **55**, 1810–1815; (*c*) H. Wang, C.-Y. Zhou and C.-M. Che, *Adv. Synth. Catal.*, 2017, **359**, 2253–2258; (*d*) F. Hao, A. R. Reddy, C.-Y. Zhou and C.-M. Che, *Adv. Synth. Catal.*, 2018, **360**, 1433–1438.

14 (*a*) G. Frenking and N. Fröhlich, *Chem. Rev.*, 2000, **100**, 717–774; (*b*) Y. Jean, *Molecular Orbitals of Transition Metal Complexes*, OUP Oxford, 2005; (*c*) J. F. Hartwig, *Organotransition Metal Chemistry: From Bonding to Catalysis*, University Science Books Sausalito, CA, 2010; (*d*) D. J. Mindiola and J. Scott, *Nat. Chem.*, 2011, **3**, 15–17.

15 J.-i. Setsune, Y. Ishimaru and A. Sera, *J. Chem. Soc. Chem. Commun.*, 1992, 328–329.

16 (*a*) Y. Liu, W. Xu, J. Zhang, W. Fuller, C. E. Schulz and J. Li, *J. Am. Chem. Soc.*, 2017, **139**, 5023–5026; (*b*) Q. Peng, J. T. Sage, Y. Liu, Z. Wang, M. Y. Hu, J. Zhao, E. E. Alp, W. R. Scheidt and J. Li, *Inorg. Chem.*, 2018, **57**, 8788–8795; (*c*) H. Wang, C. E. Schulz, X. Wei and J. Li, *Inorg. Chem.*, 2019, **58**, 143–151.

17 (*a*) N. Rajapakse, B. R. James and D. Dolphin, *Can. J. Chem.*, 1990, **68**, 2274–2277; (*b*) J. P. Collman, E. Rose and G. D. Venburg, *J. Chem. Soc. Chem. Commun.*, 1993, 934–935; (*c*) E. Galardon, P. L. Maux, L. Toupet and G. Simonneaux, *Organometallics*, 1998, **17**, 565–569; (*d*) C.-M. Che, J.-S. Huang, F.-W. Lee, Y. Li, T.-S. Lai, H.-L. Kwong, P.-F. Teng, W.-S. Lee, W.-C. Lo, S.-M. Peng and Z.-Y. Zhou, *J. Am. Chem. Soc.*, 2001, **123**, 4119–4129; (*e*) C.-M. Che and J.-S. Huang, *Coord. Chem. Rev.*, 2002, **231**, 151–164; (*f*) T. Harada, S. Wada, H. Yuge and T. K. Miyamoto, *Acta Crystallogr., Sect. C: Struct. Chem.*, 2003, **59**, m37–m39; (*g*) Y. Li, J.-S. Huang, G.-B. Xu, N. Zhu, Z.-Y. Zhou, C.-M. Che and K.-Y. Wong, *Chem.–Eur. J.*, 2004, **10**, 3486–3502; (*h*) C.-M. Che, C.-M. Ho and J.-S. Huang, *Coord. Chem. Rev.*, 2007, **251**, 2145–2166; (*i*) P. Le Maux, T. Roisnel, I. Nicolas and G. Simonneaux, *Organometallics*, 2008, **27**, 3037–3042; (*j*) K. Hirasawa, H. Yuge and T. K. Miyamoto, *Acta Crystallogr., Sect. C: Struct. Chem.*, 2008, **64**, m97–m100; (*k*) Q.-H. Deng, J. Chen, J.-S. Huang, S. S.-Y. Chui, N. Zhu, G.-Y. Li and C.-M. Che, *Chem.–Eur. J.*, 2009, **15**, 10707–10712; (*l*) H.-X. Wang, Q. Wan, K. Wu, K.-H. Low, C. Yang, C.-Y. Zhou, J.-S. Huang and C.-M. Che, *J. Am. Chem. Soc.*, 2019, **141**, 9027–9046.

18 (*a*) L. K. Woo and D. A. Smith, *Organometallics*, 1992, **11**, 2344–2346; (*b*) D. A. Smith, D. N. Reynolds and L. K. Woo, *J. Am. Chem. Soc.*, 1993, **115**, 2511–2513; (*c*) J.-P. Djukic, D. A. Smith, V. G. Young Jr and L. K. Woo, *Organometallics*, 1994, **13**, 3020–3026; (*d*) C. G. Hamaker, J.-P. Djukic, D. A. Smith and L. K. Woo, *Organometallics*, 2001, **20**, 5189–5199; (*e*) Y. Li, J.-S. Huang, Z.-Y. Zhou and C.-M. Che, *J. Am. Chem. Soc.*, 2001, **123**, 4843–4844; (*f*) Y. Li, J.-S. Huang, Z.-Y. Zhou and C.-M. Che, *Chem. Commun.*, 2003, 1362–1363; (*g*) K. Sawano, H. Yuge and T. K. Miyamoto, *Inorg. Chim. Acta*, 2005, **358**, 1830–1834.

19 (*a*) Z. Wu, S. T. Nguyen, R. H. Grubbs and J. W. Ziller, *J. Am. Chem. Soc.*, 1995, **117**, 5503–5511; (*b*) V. F. Kuznetsov, K. Abdur-Rashid, A. J. Lough and D. G. Gusev, *J. Am. Chem. Soc.*, 2006, **128**, 14388–14396.

20 (*a*) M. L. Buil, M. A. Esteruelas, C. García-Yebra, E. Gutiérrez-Puebla and M. Oliván, *Organometallics*, 2000, **19**, 2184–2193; (*b*) D. G. Gusev and A. J. Lough, *Organometallics*, 2002, **21**, 2601–2603; (*c*) R. Castro-Rodrigo, M. A. Esteruelas, S. Fuertes, A. M. López, F. López, J. L. Mascareñas, S. Mozo, E. Oñate, L. Saya and L. Villarino, *J. Am. Chem. Soc.*, 2009, **131**, 15572–15573; (*d*) R. Castro-Rodrigo, M. A. Esteruelas, A. M. López, F. López, J. L. Mascareñas, S. Mozo, E. Oñate and L. Saya, *Organometallics*, 2010, **29**, 2372–2376.

21 V. Mahias, S. Cron, L. Toupet and C. Lapinte, *Organometallics*, 1996, **15**, 5399–5408.

22 (*a*) R. A. Moss and M. J. Chang, *Tetrahedron Lett.*, 1981, **22**, 3749–3752; (*b*) T. Bally, S. Matzinger, L. Truttmann, M. S. Platz and S. Morgan, *Angew. Chem., Int. Ed.*, 1994, **33**, 1964–1966; (*c*) G. V. Shustov and M. T. H. Liu, *Can. J. Chem.*, 1998, **76**, 851–861; (*d*) W. Knoll, D. Kaneno,

M. M. Bobek, L. Brecker, M. G. Rosenberg, S. Tomoda and U. H. Brinker, *J. Org. Chem.*, 2012, **77**, 1340–1360; (*e*) V. C. Rojisha, K. Nijesh, S. De and P. Parameswaran, *Chem. Commun.*, 2013, **49**, 8465–8467; (*f*) R. A. Moss, L. Wang and K. Krogh-Jespersen, *J. Am. Chem. Soc.*, 2014, **136**, 4885–4888.

23 P. A. Chaloner, G. D. Glick and R. A. Moss, *J. Chem. Soc. Chem. Commun.*, 1983, 880–881.

24 J. Bauer, H. Braunschweig, A. Damme, J. O. C. Jimenez-Halla, T. Kramer, K. Radacki, R. Shang, E. Siedler and Q. Ye, *J. Am. Chem. Soc.*, 2013, **135**, 8726–8734.

25 V. B. Shur, I. A. Tikhonova, G. G. Aleksandrov, Y. T. Struchkov, M. E. Vol'pin, E. Schmitz and K. Jähnisch, *Inorg. Chim. Acta*, 1980, **44**, L275–L277.

26 Z. Mo and L. Deng, *Coord. Chem. Rev.*, 2017, **350**, 285–299.

27 (*a*) A. Albini and H. Kisch, *J. Organomet. Chem.*, 1975, **94**, 75–85; (*b*) R. Battaglia, H. Matthäus and H. Kisch, *J. Organomet. Chem.*, 1980, **193**, 57–67.

28 Q. Ye, I. V. Komarov, A. J. Kirby and M. Jones Jr, *J. Org. Chem.*, 2002, **67**, 9288–9294.

29 A. B. P. Lever and H. B. Gray, *Iron Porphyrins*, Addison Wesley Publishing Company, 1983.

30 (*a*) T. G. Spiro and J. M. Burke, *J. Am. Chem. Soc.*, 1976, **98**, 5482–5489; (*b*) G. Chottard and D. Mansuy, *J. Chem. Soc. Chem. Commun.*, 1980, 279–280; (*c*) G. Chottard, P. Battioni, J.-P. Battioni, M. Lange and D. Mansuy, *Inorg. Chem.*, 1981, **20**, 1718–1722.

31 (*a*) J.-S. Huang, C.-M. Che and C.-K. Poon, *J. Chem. Soc. Chem. Commun.*, 1992, 161–163; (*b*) J.-L. Liang, J.-S. Huang, Z.-Y. Zhou, K.-K. Cheung and C.-M. Che, *Chem.–Eur. J.*, 2001, **7**, 2306–2317.

32 A. Antipas, J. W. Buchler, M. Gouterman and P. D. Smith, *J. Am. Chem. Soc.*, 1978, **100**, 3015–3024.

33 D. Lancon and K. M. Kadish, *J. Am. Chem. Soc.*, 1983, **105**, 5610–5617.

34 (*a*) K. M. Kadish, E. Van Caemelbecke, F. D'Souza, M. Lin, D. J. Nurco, C. J. Medforth, T. P. Forsyth, B. Krattinger, K. M. Smith, S. Fukuzumi, I. Nakanishi and J. A. Shelnutt, *Inorg. Chem.*, 1999, **38**, 2188–2198; (*b*) K. T. Moore, J. T. Fletcher and M. J. Therien, *J. Am. Chem. Soc.*, 1999, **121**, 5196–5209.

35 (*a*) G. M. Brown, F. R. Hopf, J. A. Ferguson, T. J. Meyer and D. G. Whitten, *J. Am. Chem. Soc.*, 1973, **95**, 5939–5942; (*b*) T. Malinski, D. Chang, L. A. Bottomley and K. M. Kadish, *Inorg. Chem.*, 1982, **21**, 4248–4253; (*c*) I.-K. Choi, Y. Liu, D. Feng, K.-J. Paeng and M. D. Ryan, *Inorg. Chem.*, 1991, **30**, 1832–1839.

36 (*a*) G. M. Brown, F. R. Hopf, T. J. Meyer and D. G. Whitten, *J. Am. Chem. Soc.*, 1975, **97**, 5385–5390; (*b*) J. P. Collman, J. T. McDevitt, C. R. Leidner, G. T. Yee, J. B. Torrance and W. A. Little, *J. Am. Chem. Soc.*, 1987, **109**, 4606–4614.

37 R. L. Khade, W. Fan, Y. Ling, L. Yang, E. Oldfield and Y. Zhang, *Angew. Chem., Int. Ed.*, 2014, **53**, 7574–7578.

38 C. J. Ziegler and K. S. Suslick, *J. Am. Chem. Soc.*, 1996, **118**, 5306–5307.

39 (*a*) C. Werlé, R. Goddard and A. Fürstner, *Angew. Chem., Int. Ed.*, 2015, **54**, 15452–15456; (*b*) C. Werlé, R. Goddard, P. Philipps, C. Farès and A. Fürstner, *J. Am. Chem. Soc.*, 2016, **138**, 3797–3805.

40 (*a*) X. Dai and T. H. Warren, *J. Am. Chem. Soc.*, 2004, **126**, 10085–10094; (*b*) P. Hofmann, I. V. Shishkov and F. Rominger, *Inorg. Chem.*, 2008, **47**, 11755–11762.

41 (*a*) C. Soldi, K. N. Lamb, R. A. Squitieri, M. González-López, M. J. Di Maso and J. T. Shaw, *J. Am. Chem. Soc.*, 2014, **136**, 15142–15145; (*b*) D. Zhu, J. Ma, K. Luo, H. Fu, L. Zhang and S. Zhu, *Chem. Commun.*, 2016, **55**, 8452–8456; (*c*) L. W. Souza, R. A. Squitieri, C. A. Dimirjian, B. M. Hodur, L. A. Nickerson, C. N. Penrod, J. Cordova, J. C. Fettinger and J. T. Shaw, *Angew. Chem., Int. Ed.*, 2018, **57**, 15213–15216; (*d*) D. Zhu, L. Chen, H. Zhang, Z. Ma, H. Jiang and S. Zhu, *Angew. Chem., Int. Ed.*, 2018, **57**, 12405–12409.

42 (*a*) D. A. Sharon, D. Mallick, B. Wang and S. Shaik, *J. Am. Chem. Soc.*, 2016, **138**, 9597–9610; (*b*) Y. Wei, A. Tinoco, V. Steck, R. Fasan and Y. Zhang, *J. Am. Chem. Soc.*, 2018, **140**, 1649–1662.

43 (*a*) J. R. Denton, D. Sukumaran and H. M. L. Davies, *Org. Lett.*, 2007, **9**, 2625–2628; (*b*) P. Rullière, G. Benoit, E. M. D. Allouche and A. B. Charette, *Angew. Chem., Int. Ed.*, 2018, **57**, 5777–5782; (*c*) E. M. D. Allouche and A. B. Charette, *Chem. Sci.*, 2019, **10**, 3802–3806.

44 G.-Q. Chen, Z.-J. Xu, C.-Y. Zhou and C.-M. Che, *Chem. Commun.*, 2011, **47**, 10963–10965.

45 (*a*) P. Q. Le and J. A. May, *J. Am. Chem. Soc.*, 2015, **137**, 12219–12222; (*b*) Y. Wang, X. Wen, X. Cui and X. P. Zhang, *J. Am. Chem. Soc.*, 2018, **140**, 4792–4796; (*c*) J. Werth and C. Uyeda, *Angew. Chem., Int. Ed.*, 2018, **57**, 13902–13906; (*d*) M. Lankelma, A. M. Olivares and B. de Bruin, *Chem.–Eur. J.*, 2019, **25**, 5658–5663; (*e*) S. Yu, A. Noble, R. B. Bedford and V. K. Aggarwal, *J. Am. Chem. Soc.*, 2019, **141**, 20325–20334.

46 D. Munz, *Organometallics*, 2018, **37**, 275–289.

47 D. Bourissou, O. Guerret, F. P. Gabbaï and G. Bertrand, *Chem. Rev.*, 2000, **100**, 39–92.

48 C. M. Weinstein, G. P. Junor, D. R. Tolentino, R. Jazzar, M. Melaimi and G. Bertrand, *J. Am. Chem. Soc.*, 2018, **140**, 9255–9260.

49 (*a*) C. Samojłowicz, M. Bieniek and K. Grela, *Chem. Rev.*, 2009, **109**, 3708–3742; (*b*) T. Hashimoto, S. Urban, R. Hoshino, Y. Ohki, K. Tatsumi and F. Glorius, *Organometallics*, 2012, **31**, 4474–4479; (*c*) P. Stefan and W. Robert, *Z. Anorg. Allg. Chem.*, 2013, **639**, 2581–2585; (*d*) K.-H. Chan, X. Guan, V. K.-Y. Lo and C.-M. Che, *Angew. Chem., Int. Ed.*, 2014, **53**, 2982–2987; (*e*) P. P. Samuel, K. C. Mondal, N. A. Sk, H. W. Roesky, E. Carl, R. Neufeld, D. Stalke, S. Demeshko, F. Meyer, L. Ungur, L. F. Chibotaru, J. Christian, V. Ramachandran, J. van Tol and N. S. Dalal, *J. Am. Chem. Soc.*, 2014, **136**, 11964–11971; (*f*) G. Ung, J. Rittle, M. Soleilhavoup, G. Bertrand and J. C. Peters, *Angew. Chem., Int. Ed.*, 2014, **53**, 8427–8431; (*g*) G. Ung and J. C. Peters, *Angew. Chem., Int. Ed.*, 2015, **54**, 532–535; (*h*) V. M. Marx, A. H. Sullivan, M. Melaimi, S. C. Virgil, B. K. Keitz, D. S. Weinberger, G. Bertrand and R. H. Grubbs, *Angew. Chem., Int. Ed.*, 2015, **54**, 1919–1923; (*i*) L. Wang, L. Hu, H. Zhang, H. Chen and L. Deng, *J. Am.*

Chem. Soc., 2015, **137**, 14196–14207; (*j*) K.-P. Shing, Y. Liu, B. Cao, X.-Y. Chang, T. You and C.-M. Che, *Angew. Chem., Int. Ed.*, 2018, **57**, 11947–11951.

50 G. Dazinger and K. Kirchner, *Organometallics*, 2004, **23**, 6281–6287.

51 L. W. Olson, D. Schaeper, D. Lancon and K. M. Kadish, *J. Am. Chem. Soc.*, 1982, **104**, 2042–2044.

52 B. B. Wayland, L. F. Mehne and J. Swartz, *J. Am. Chem. Soc.*, 1978, **100**, 2379–2383.

53 G. B. Jameson and J. A. Ibers, *Inorg. Chem.*, 1979, **18**, 1200–1208.

54 L. A. Bottomley, M. R. Deakin and J.-N. Gorce, *Inorg. Chem.*, 1984, **23**, 3563–3571.

55 (*a*) W. Baratta, W. A. Herrmann, R. M. Kratzer and P. Rigo, *Organometallics*, 2000, **19**, 3664–3669; (*b*) H. Werner, M. E. Schneider, M. Bosch, J. Wolf, J. H. Teuben, A. Meetsma and S. I. Troyanov, *Chem.–Eur. J.*, 2000, **6**, 3052–3059; (*c*) S. Priya, M. S. Balakrishna, S. M. Mobin and R. McDonald, *J. Organomet. Chem.*, 2003, **688**, 227–235; (*d*) A. Hamze, B. Tréguier, J.-D. Brion and M. Alami, *Org. Biomol. Chem.*, 2011, **9**, 6200–6204; (*e*) H. Liu, Y. Wei and C. Cai, *New J. Chem.*, 2016, **40**, 674–678; (*f*) Z. Liu, Q. Li, Y. Yang and X. Bi, *Chem. Commun.*, 2017, **53**, 2503–2506.

56 R. M. Parrish and C. D. Sherrill, *J. Am. Chem. Soc.*, 2014, **136**, 17386–17389.